

Air Force Institute of Technology

AFIT Scholar

Theses and Dissertations

Student Graduate Works

3-10-2008

Modulation Response of Twin Optically Coupled Diode Lasers

Eric M. Golden

Follow this and additional works at: <https://scholar.afit.edu/etd>



Part of the [Plasma and Beam Physics Commons](#)

Recommended Citation

Golden, Eric M., "Modulation Response of Twin Optically Coupled Diode Lasers" (2008). *Theses and Dissertations*. 2717.

<https://scholar.afit.edu/etd/2717>

This Thesis is brought to you for free and open access by the Student Graduate Works at AFIT Scholar. It has been accepted for inclusion in Theses and Dissertations by an authorized administrator of AFIT Scholar. For more information, please contact richard.mansfield@afit.edu.



MODULATION RESPONSE
OF
TWIN OPTICALLY COUPLED
DIODE LASERS

THESIS

Eric M. Golden, Captain, USAF

AFIT/GAP/ENP/08-M05

DEPARTMENT OF THE AIR FORCE
AIR UNIVERSITY

AIR FORCE INSTITUTE OF TECHNOLOGY

Wright-Patterson Air Force Base, Ohio

APPROVED FOR PUBLIC RELEASE; DISTRIBUTION UNLIMITED

The views expressed in this thesis are those of the author and do not reflect the official policy or position of the United States Air Force, Department of Defense, or the United States Government.

AFIT/GAP/ENP/08-M05

MODULATION RESPONSE
OF
TWIN OPTICALLY COUPLED
DIODE LASERS

THESIS

Presented to the Faculty
Department of Engineering Physics
Graduate School of Engineering and Management
Air Force Institute of Technology
Air University
Air Education and Training Command
In Partial Fulfillment of the Requirements for the
Degree of Master of Science

Eric M. Golden, BS
Captain, USAF

27 March 2008

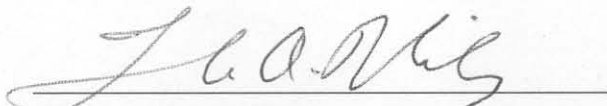
APPROVED FOR PUBLIC RELEASE; DISTRIBUTION UNLIMITED

AFIT/GAP/ENP/08-M05


MODULATION RESPONSE
OF
TWIN OPTICALLY COUPLED
DIODE LASERS

Eric M. Golden, BS
Captain, USAF

Approved:


Thomas Niday (Chairman)

5 Mar 2008
Date


Vassilios Kovanis (Member)

10 Mar 2008
Date


Matthew Bohn (Member)

5 Mar 2008
Date

Abstract

Diode lasers are useful in military and commercial applications that have strict requirements for size, weight and power. This includes the use of diode lasers in optoelectronic and photonic integrated circuits, which can lead to new technologies in optical communications and optical interconnects in high performance computing systems. For these systems to be effective, the diode laser must be modulated at frequencies beyond current limits which are typically a few GHz. This barrier can be broken by optically coupling a diode laser with a similar laser.

A set of single mode rate equations models the dynamics of twin optically coupled diode lasers. Steady states of the system are derived analytically or calculated numerically when an analytic expression is not easily available. The stability of the steady states is examined by using a linear stability analysis, which is also used in an algorithm that calculates the infinitesimal modulation response. The modulation response is also calculated by using a numerical method that directly integrates the rate equations. Typical parameters for an InGaAsP diode laser are used in the algorithms to investigate mutual coupling and evanescent coupling. It will be shown that mutually coupled lasers can be effectively modulated out to frequencies of approximately 9 GHz compared to 4 GHz for a solitary laser. For evanescent coupling, the steady states are unstable over large regions of the parameter space, but this is remedied by introducing asymmetric DC currents through the lasers or by introducing the effects of gain saturation. With stable steady states, evanescently coupled lasers can be effectively modulated at frequencies out to about 30 GHz which is more than a seven fold improvement over a solitary laser.

Acknowledgements

I would like to thank my wife and our daughter for their love and support over the past year and a half. I would also like to thank Dr. Kovanis and Maj. Niday for their wisdom and guidance.

Table of Contents

	Page
Abstract	iv
Acknowledgements	v
List of Figures	vii
List of Tables	ix
List of Symbols	x
I. Introduction	1
II. Theory	5
2.1 Rate Equations	5
2.2 Model of Twin Optically Coupled Diode Lasers	10
2.3 Modulation Response of a Solitary Diode Laser	14
III. Computational Methods	20
3.1 Linear Stability Analysis	20
3.2 Infinitesimal Modulation Response	21
3.3 Non-linear Modulation Response	23
IV. Simulations	26
4.1 Mutual Coupling	26
4.2 Evanescent Coupling	29
4.2.1 Asymmetric Pumping Stabilization	32
4.2.2 Gain Saturation Stabilization	36
V. Summary and Conclusions	41
Appendix A. Steady States for Mutual Coupling	44
Appendix B. Steady States for Evanescent Coupling	50
Appendix C. ModulationResponse.m	55
Appendix D. NUMOR Source Code	58
Appendix E. SteadyState.m	69
Bibliography	74

List of Figures

Figure		Page
1.	Some properties of the modulation response for a solitary InGaAsP diode laser.....	2
2.	Twin optically coupled diode lasers	4
3.	Lasing in a diode laser	6
4.	Modulation response of a solitary InGaAsP diode laser	19
5.	Regions of stability for symmetric steady states of mutual coupling with symmetric pumping rates and a steady state phase difference of zero.	27
6.	Modulation response of twin mutually coupled InGaAsP diode lasers at several coupling strengths	28
7.	Modulation response of twin evanescently coupled InGaAsP diode lasers with unstable steady states, and the time evolution of the electric field with no modulation.....	30
8.	Regions of stability for symmetric steady states of evanescent coupling with symmetric pumping rates	31
9.	Damping coefficients vs. current displacement.	34
10.	Modulation response of evanescently coupled InGaAsP diode lasers with a current displacement of 28.4 mA.	35
11.	Regions of stability for symmetric steady states of evanescent coupling with symmetric pumping rates and gain saturation	38
12.	Damping coefficients vs. dimensionless gain saturation coefficient. ...	39
13.	Modulation response of twin evanescently coupled InGaAsP diode lasers with a dimensionless gain coefficient of 0.03.	40
14.	Non-linear modulation response of twin mutually coupled InGaAsP diode lasers	42
15.	Regions of stability for symmetric steady states of mutual coupling with symmetric pumping rates	47
16.	Regions of stability and existence for asymmetric steady states of mutual coupling with symmetric pumping rates	49

Figure		Page
17.	Regions of stability for symmetric steady states of evanescent coupling with symmetric pumping rates	53
18.	Regions of stability and existence for asynchronous steady states of evanescent coupling with synchronous pumping rates	54

List of Tables

Table		Page
1.	Parameters for a $1.3 \mu m$ buried-heterostructure InGaAsP diode laser .	10
2.	Dimensionless conversion coefficients	12
3.	Typical model parameters	14

List of Symbols

Symbol		Page
t	Time (s)	5
S	Photon density (cm^{-3})	5
G	Gain (s^{-1})	5
R_{sp}	Spontaneous emission rate into the lasing mode ($\text{cm}^{-3}\text{s}^{-1}$)	5
τ_p	Photon lifetime (s)	6
N	Carrier density (cm^{-3})	6
P	Electrical pumping rate ($\text{cm}^{-3}\text{s}^{-1}$)	6
τ_c	Carrier lifetime (s)	6
G_{th}	Threshold gain (s^{-1})	7
G_N	Differential gain (cm^3/s)	7
N_{th}	Threshold carrier density (cm^{-3})	7
\mathcal{E}	Electric field (statvolt/cm)	8
c	Speed of light in a vacuum (cm/s)	8
ϵ	Relative permittivity	8
E	Slowly varying electric field	8
ω	Angular frequency of the lasing mode	8
k	Effective mode propagation constant	8
$\psi(x, y)$	Transverse electric field distribution within the laser	8
$\langle \epsilon \rangle$	Averaged relative permittivity	8
n_r	Real part of the effective mode index	9
n_i	Imaginary part of the effective mode index	9
δ	Indicates a small deviation	9
α	Line-width enhancement factor	9
κ	Optical coupling term	11
τ_{in}	Round trip time in the laser cavity	11
τ	Time delay	11

Symbol		Page
\hat{E}	Dimensionless slowly varying electric field	11
\hat{N}	Dimensionless excess carrier density	11
\hat{t}	Dimensionless time	11
\hat{P}	Dimensionless excess electrical pumping rate	11
P_{th}	Threshold electrical pumping rate	11
T	Ratio of the carrier lifetime to the photon lifetime	11
R	Dimensionless slowly varying electric field amplitude	12
θ	Slowly varying electric field phase	12
η	Dimensionless optical coupling strength	12
ϕ	Optical coupling phase	12
Θ	Slowly varying electric field phase difference	13
\hat{N}_s	Steady state dimensionless excess carrier density	15
R_s	Steady state dimensionless slowly varying electric field amplitude	15
\hat{P}_s	Steady state dimensionless excess electrical pumping rate	15
θ_s	Steady state slowly varying electric field phase	15
γ_r	Dimensionless relaxation damping coefficient	16
ω_r	Dimensionless relaxation oscillation frequency	17
$\mathcal{F}\{\}$	Fourier transform operator	17
ω_m	Dimensionless angular modulation frequency	17
M	Modulation response	17
J	Jacobian matrix	18
I	Identity matrix	18
Δ	Dimensionless excess electrical pumping rate displacement	32
β	Gain saturation coefficient	36
$\hat{\beta}$	Dimensionless gain saturation coefficient	36

MODULATION RESPONSE OF TWIN OPTICALLY COUPLED DIODE LASERS

I. Introduction

Diode lasers are useful in high speed optical communications, as well as long-haul terrestrial and transoceanic communications [1; 2]. Because of their small size and high efficiency, they are also useful in UAV and satellite payloads, as well as in other remote tactical applications that have strict requirements on size, weight and power [1]. Diode lasers undergoing optical feedback or injection can be driven into chaos. In this state diode lasers can be used for secure transmission of information [3; 4]. Diode lasers can also play an important role in optoelectronic and photonic integrated circuits as small efficient sources of photons [5]. These optoelectronic and photonic devices can possibly lead to the next generation of communications and computing devices, where the circuitry makes use of photons instead of electrons to process information and perform computations.

In order to transmit information, the output of the diode laser must be modulated. This is commonly achieved in diode lasers by varying the electrical current through the laser [6]. The diode laser must be effectively modulated at high frequencies for fast transmission of information. While diode lasers are small, light and efficient, they typically do not perform effectively when modulated at frequencies beyond the relaxation oscillation frequency, which is typically a few gigahertz [6]. However, it has been shown in experiments [7; 8] and theory [1; 2; 6] that diode lasers can be effectively modulated beyond the frequency of relaxation oscillations when optically injected or optically coupled with similar diode lasers. Because of this, the

modulation characteristics of coupled diode lasers have become a topic of interest [7; 8; 9; 10; 11; 12].

The modulation characteristics of a diode laser are examined by studying the modulation response. The modulation response of a diode laser is defined as the ratio of the modulated electric field amplitude to the modulated electrical current amplitude through the laser normalized to the response at a modulation frequency of zero [1; 13]. From the modulation response, characteristics such as bandwidth and peak response are extracted. Figure 1 shows some features of the modulation response of a solitary diode laser. For communications and other applications, the bandwidth should be broad, which allows more information to be transmitted, and the modulation response as flat as possible across the bandwidth in order to avoid having the band dominated by one or possibly a few modulation frequencies.

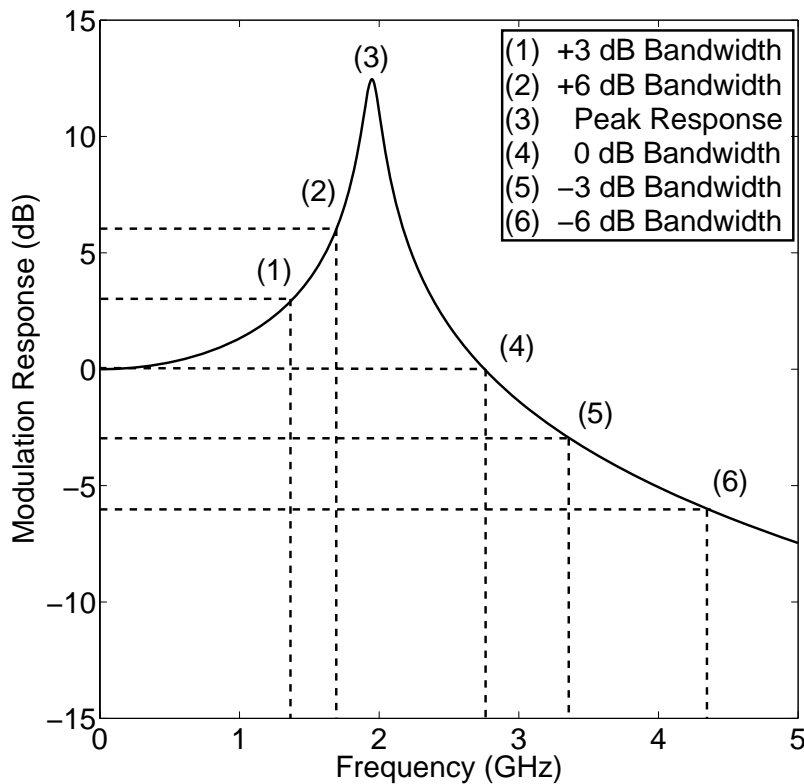
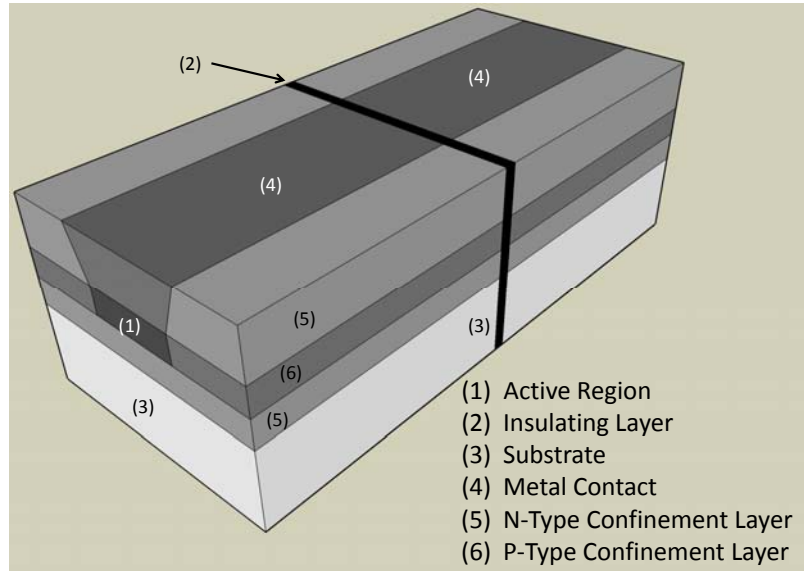


Figure 1. Some properties of the modulation response for a solitary InGaAsP diode laser. Adapted from Reference [1] and Reference [14].

In order to calculate the modulation response, the dynamics of the laser must be studied. The first step is to derive [13; 14; 15] an appropriate set of rate equations. For a solitary laser, a set of equations that describe the loss and gain of photons as well as the loss and gain of electrons in the gain medium is sufficient [14]. However, the model of a coupled laser system must account for the electric field amplitude and phase, since the electric fields of the twin lasers must be coherently added [16]. In Section 2.1, a rate equation for the complex slowly varying electric field is formulated and used in Section 2.2 to develop a model for a system of twin optically coupled diode lasers [11; 12]. The model is then applied to a solitary laser in Section 2.3. This will establish a performance baseline for the coupled system as well as define some terms commonly used in this field of study. The treatment used for the solitary laser is then used in Chapter III to develop a set of computational methods that determine the stability of the steady states (Section 3.1), compute the infinitesimal modulation response (Section 3.2), and numerically compute the modulation response (Section 3.3). Next, these computational methods are used in Chapter IV to simulate two cases of optical coupling (Figure 2). First in Section 4.1, where the lasers are mutually coupled (Figure 2a) by directly injecting photons through the output couplers [17] and second where photons are passed through the sides of the lasers (Figure 2b) by way of an evanescent wave [1; 6; 18; 19]. It is shown in this document that the bandwidth of mutually coupled lasers is slightly enhanced when modulated in-phase with the same signal, but when modulated out-of-phase the response becomes flatter. It is also shown in this document that the modulation bandwidth of evanescently coupled diode lasers is about six times that of a solitary laser when the coupled lasers are modulated out-of-phase with the same signal.

(a) Mutually Coupled Diode Lasers



(b) Evanescently Coupled Diode Lasers

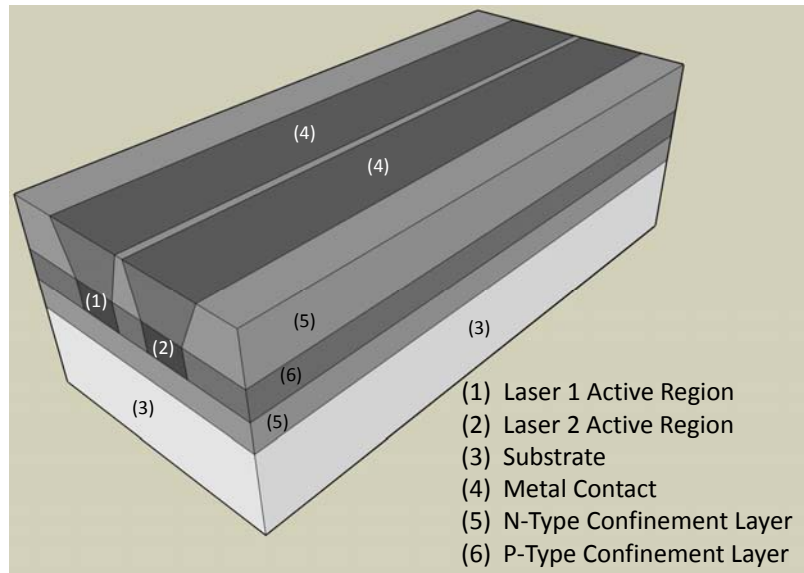


Figure 2. (a) Mutually coupled buried-heterostructure twin diode lasers. Between the lasers the photons couple out of the output couplers and into the output couplers of the other laser. (b) Evanescently coupled buried-heterostructure twin diode lasers. The confinement layers set up the lasing mode through total internal reflection. When the lasers are close enough together the evanescent waves in each laser will couple into the lasing mode of the other. Adapted from Reference [13] and Reference [20].

II. Theory

In this document single mode rate equations are used to model the dynamics of twin optically coupled diode lasers. Because of this, it is important to understand how these rate equations are derived. The first step is to examine a standard set of rate equations for solitary diode lasers [14; 21]. These standard equations describe the photon and carrier densities in the diode laser, but in order to model an optically coupled system, rate equations for the electric field amplitude and phase must be derived [13]. Once this is complete, the model for a coupled system is developed. Finally, the model is applied to a solitary laser, which establishes a performance baseline and leads into the development of computational methods for the coupled system.

2.1 Rate Equations

Diode laser systems are modeled by a set of rate equations that describe the exchange of carriers and photons [14; 21]. The rate equation for the photon density is

$$\frac{dS}{dt} = G(N, S)S(t) + R_{sp} - \frac{S(t)}{\tau_p}, \quad (1)$$

and includes terms that account for gains in photons due to spontaneous and stimulated emission and losses due to absorption and output coupling. The rate equation for the carrier density is

$$\frac{dN}{dt} = P(t) - \frac{N(t)}{\tau_c} - G(N, S)S(t), \quad (2)$$

and includes terms that account for gain due to pumping and losses due to stimulated emission, spontaneous emission and non-radiative transitions. In Equations (1,2) t is time in seconds, S is the photon density in cm^{-3} , G is net gain per second, and R_{sp} is the rate of photons that are spontaneously emitted into the lasing mode in

$\text{cm}^{-3}\text{s}^{-1}$. The term that includes the photon lifetime in seconds (τ_p) accounts for the loss of photons due to absorption and output coupling. The term that includes the carrier density in cm^{-3} (N) accounts for the number of electron-hole pairs in the active region. The electrical pumping rate in $\text{cm}^{-3}\text{s}^{-1}$ (P) is proportional to the current density through the diode laser. The term that includes the carrier lifetime in seconds (τ_c) accounts for electron-hole recombination for both radiative and non-radiative transitions. Figure 3 illustrates the processes in a diode laser that are described by the rate equations.

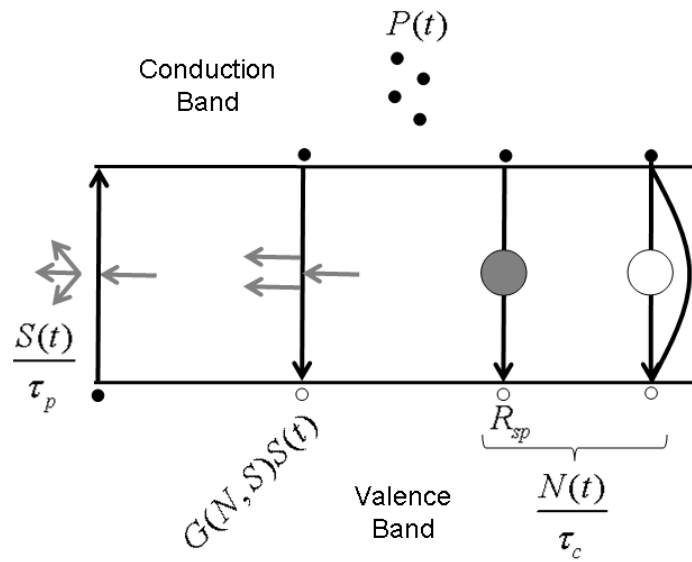


Figure 3. Lasing in a diode laser. Gray arrows indicate photons that contribute to the lasing mode. Solid black circles indicate electrons (carriers). Hollow black circles indicate holes. The large gray circle indicates spontaneously emitted photons in the lasing mode. The large hollow circle indicates spontaneously emitted photons not in the lasing mode and the curved black line indicates non-radiative transitions. Downward pointing black arrows indicate electron hole recombination and the upward pointing black arrow indicates electron promotion to the conduction band through photon absorption.

If the photon density is assumed to be at a level where gain saturation effects are minimal, then a linear model of gain [14; 22] can be used. The linear gain model

is

$$G(N) = G_{th} + G_N(N - N_{th}) = \frac{1}{\tau_p} + G_N(N - N_{th}), \quad (3)$$

where G_{th} is the threshold gain with units of s^{-1} , G_N is the differential gain with units of cm^3/s , and N_{th} is the threshold carrier density. Since $\frac{S(t)}{\tau_p}$ accounts for all losses in the lasing mode, the threshold gain equals $\frac{1}{\tau_p}$. If the number of photons in the lasing mode is primarily due to stimulated emission, which is typically the case while operating above threshold, then the rate of spontaneous emission into the lasing mode can be ignored. With this assumption and the linear gain model, Equations (1,2) become

$$\frac{dS}{dt} = G_N(N - N_{th})S(t) \quad (4)$$

$$\frac{dN}{dt} = P(t) - \frac{N(t)}{\tau_c} - \left(\frac{1}{\tau_p} + G_N(N - N_{th})\right)S(t). \quad (5)$$

This set of rate equations can be used to model the dynamics of a solitary diode laser, but in order to model coupled diode lasers the fields created by stimulated emission and the fields created by coupling within each laser must be coherently added. This requires rate equations for the electric fields in each laser. The place to start for these rate equations is Maxwell's wave equation [13; 14; 15].

The following derivation follows Agrawal and Dutta's treatment in Reference [13]. Assuming propagation along an arbitrary z-axis, non-conductive and nonmagnetic materials, instantaneous changes in the polarization field, and single mode operation, the wave equation for the electric field is written as

$$\frac{\partial^2 \mathcal{E}(x, y, z, t)}{\partial z^2} = \epsilon \frac{1}{c^2} \frac{\partial^2 \mathcal{E}(x, y, z, t)}{\partial t^2}, \quad (6)$$

where \mathcal{E} is the electric field in Gaussian units, c is the speed of light in a vacuum, and ϵ is the relative permittivity. The electric field is written as

$$\mathcal{E}(x, y, z, t) = \psi(x, y) \sin(kz)E(t)e^{-i\omega t}, \quad (7)$$

where E is the slowly varying electric field, ω is the angular frequency of the lasing mode, and k is the effective mode propagation constant. The transverse electric field distribution is represented by $\psi(x, y)$ while $\sin(kz)$ accounts for the electric field distribution along the direction of propagation created by the Fabry-Perot cavity [13]. Substituting Equation (7) into Equation (6) and ignoring second derivatives of E , since it is assumed to be slowly varying, yields

$$-k^2\psi(x, y) \sin(kz)E(t) = \epsilon\psi(x, y) \sin(kz) \left(-\frac{2i\omega}{c^2} \frac{\partial E}{\partial t} - \frac{\omega^2}{c^2} E(t) \right). \quad (8)$$

The spatial dependence of Equation (8) is handled by multiplying Equation (8) by $\psi(x, y) \sin(kz)$ and integrating across all x , y , and z . Assuming that $\psi(x, y) \sin(kz)$ is properly normalized such that

$$\int \int \int \psi(x, y)^2 \sin^2(kz) dx dy dz = 1, \quad (9)$$

Equation (8) becomes

$$-\langle \epsilon \rangle \frac{2i\omega}{c^2} \frac{\partial E}{\partial t} = \left(\langle \epsilon \rangle \frac{\omega^2}{c^2} - k^2 \right) E(t), \quad (10)$$

where

$$\langle \epsilon \rangle = \int \int \int \epsilon(x, y) \psi(x, y)^2 \sin^2(kz) dx dy dz.$$

Since the electric field will most likely be dispersed across several materials, ϵ may not be constant across the laser. This is the reason for $\langle \epsilon \rangle$, which is a weighted average of relative permittivities across the areas where there is an electric field and can be

approximated as the square of the effective mode index. While lasing, the carrier density is pinned at its threshold value as well as the gain. This means that the relative permittivity is real at threshold, and any deviations in the carrier density will lead to a change in relative permittivity [15]. This is accounted for with

$$\begin{aligned}\langle \epsilon \rangle &= (n_r + \delta n_r + i\delta n_i)^2 \\ &\approx n_r^2 + 2in_r\delta n_i(1 - i\alpha),\end{aligned}\quad (11)$$

where

$$\alpha = \frac{\delta n_r}{\delta n_i}. \quad (12)$$

In Equation (11), n_r is the real part of the effective mode index, n_i is the imaginary part of the effective mode index, δ indicates small deviations, and α is the line-width enhancement factor [15]. Since

$$k \approx n_r \frac{\omega}{c}, \quad (13)$$

Equation (10) is written as

$$\frac{\partial E}{\partial t} = -\frac{\omega\delta n_i}{n_r}E(t). \quad (14)$$

The imaginary part of the refractive index is related to net gain through

$$\frac{1}{2}(G(N, E) - \frac{1}{\tau_p}) = -\frac{\omega\delta n_i}{n_r}. \quad (15)$$

With Equation (15) and using the linear gain model in Equation (3), Equation (14) is written as

$$\frac{\partial E}{\partial t} = \frac{1}{2}(1 - i\alpha)G_N(N - N_{th})E(t), \quad (16)$$

which is the rate equation for the slowly varying electric field. Since the square of the absolute value of the slowly varying electric field is proportional to the intensity and intensity is proportional to the photon density, the electric field can be normalized such that $S = EE^*$. With this normalization, the rate equations for the slowly varying electric field and carrier density become

$$\frac{dE}{dt} = \frac{1}{2}(1 - i\alpha)G_N(N - N_{th})E(t) \quad (17)$$

$$\frac{dN}{dt} = P(t) - \frac{N(t)}{\tau_c} - \left(\frac{1}{\tau_p} + G_N(N - N_{th})\right)|E(t)|^2. \quad (18)$$

Table 1 shows some typical values of the parameters in Equations (17, 18). These equations can be used to model a solitary laser, but an additional term will need to be added to Equation (17) in order to model diode lasers undergoing optical injection or feedback. This is converted in the next section where the model for twin optically coupled diode lasers is developed.

Table 1. Parameters for a 1.3 μm buried-heterostructure InGaAsP diode laser [13].

Name	Symbol	Value	Units
Line-width Enhancement Factor	α	5	-
Carrier Lifetime	τ_c	2.2	ns
Photon Lifetime	τ_p	1.6	ps
Time in Cavity	τ_{in}	2.8	ps
Differential Gain	G_N	6.6×10^{-7}	cm^3/s
Threshold Carrier Density	N_{th}	1.0×10^{18}	cm^{-3}
Threshold Current	-	15.8	mA
Cavity Length	-	250	μm
Active Region Width	-	2	μm
Active Region Thickness	-	0.2	μm
Effective Mode Index	-	3.4	-

2.2 Model of Twin Optically Coupled Diode Lasers

A diode laser undergoing optical injection or feedback is modeled by a modified version of the rate equations derived in Section 2.1. Lang and Kobayashi show that

the rate equation for the electric field needs an additional term in order to account for optical injection or feedback [16]. The modified rate equations are

$$\frac{dE}{dt} = \frac{1}{2}(1 - i\alpha)G_N(N - N_{th})E(t) + \frac{\kappa}{\tau_{in}}E_{inj}(t - \tau) \quad (19)$$

$$\frac{dN}{dt} = P(t) - \frac{N(t)}{\tau_c} - \left(\frac{1}{\tau_p} + G_N(N - N_{th})\right)|E(t)|^2, \quad (20)$$

where κ is the optical coupling term, τ_{in} is the time that a photon takes to transverse the laser cavity twice, and τ is the time delay of the optical injection or feedback. For convenience, Equations(19,20) are transformed into dimensionless form [22; 23] by introducing

$$\begin{aligned} \hat{E} &\equiv \sqrt{\frac{\tau_c G_N}{2}} E \\ \hat{N} &\equiv \frac{\tau_p G_N}{2} (N - N_{th}) \\ \hat{t} &\equiv \frac{t}{\tau_p} \\ \hat{P} &\equiv \frac{\tau_p G_N N_{th}}{2} \left(\frac{P}{P_{th}} - 1 \right) \\ P_{th} &= \frac{N_{th}}{\tau_c} \\ T &\equiv \frac{\tau_c}{\tau_p} \\ \hat{\kappa} &\equiv \frac{\kappa \tau_p}{\tau_{in}} \\ \hat{\tau} &\equiv \frac{\tau}{\tau_p}. \end{aligned} \quad (21)$$

In these equations, \hat{E} is the dimensionless slowly varying electric field, \hat{N} is the dimensionless excess carrier density, \hat{t} is dimensionless time, \hat{P} is the dimensionless excess electrical pumping rate, P_{th} is the threshold electrical pumping rate, and T is the ratio of the carrier lifetime to the photon lifetime. Table 2 shows some values of the coefficients in Equation (21) using values from Table 1. The rate equations in terms of the new variables in Equation (21) now become

$$\frac{d\hat{E}}{d\hat{t}} = (1 - i\alpha)\hat{N}(\hat{t})\hat{E}(\hat{t}) + \hat{\kappa}\hat{E}_{inj}(\hat{t} - \hat{\tau}) \quad (22)$$

$$\frac{d\hat{N}}{d\hat{t}} = \hat{P}(\hat{t}) - \hat{N}(\hat{t}) - (1 + 2\hat{N}(\hat{t}))|\hat{E}(\hat{t})|^2. \quad (23)$$

Table 2. Dimensionless conversion coefficients using values from Table 1.

Coefficient	Value	Units
$\sqrt{\tau_c G_N}/2$	2.7×10^{-8}	$\text{cm}^{3/2}$
$\tau_p G_N/2$	5.3×10^{-19}	cm^3
$\tau_p G_N N_{th}/2$	0.53	—
T	1375	—
τ_p/τ_{in}	0.57	—

For a twin optically coupled diode laser system each laser is modeled by Equations (22,23) with the output of each laser injecting into the other as shown in the following equations:

$$\frac{d\hat{E}_1}{d\hat{t}} = (1 - i\alpha)\hat{N}_1\hat{E}_1 + \hat{\kappa}\hat{E}_2(\hat{t} - \hat{\tau}) \quad (24)$$

$$\frac{d\hat{E}_2}{d\hat{t}} = (1 - i\alpha)\hat{N}_2\hat{E}_2 + \hat{\kappa}\hat{E}_1(\hat{t} - \hat{\tau}) \quad (25)$$

$$T\frac{d\hat{N}_1}{d\hat{t}} = \hat{P}_1 - \hat{N}_1 - (1 + 2\hat{N}_1)|\hat{E}_1|^2 \quad (26)$$

$$T\frac{d\hat{N}_2}{d\hat{t}} = \hat{P}_2 - \hat{N}_2 - (1 + 2\hat{N}_2)|\hat{E}_2|^2. \quad (27)$$

Since both \hat{E} and $\hat{\kappa}$ are complex, Equations (24-27) are decomposed into real and imaginary parts by substituting

$$\hat{E}(\hat{t}) = R(\hat{t})e^{i\theta(\hat{t})} \quad (28)$$

$$\hat{\kappa} = \eta e^{i\phi}, \quad (29)$$

where R is the dimensionless slowly varying electric field amplitude, θ is the slowly varying electric field phase, η is the dimensionless coupling strength, and ϕ is the coupling phase. After substitution Equations (24,25) are decomposed into their am-

plitude and phase parts as shown in the following equations:

$$\frac{dR_1}{d\hat{t}} = \hat{N}_1 R_1 + \eta R_2 (\hat{t} - \hat{\tau}) \cos(\theta_2 (\hat{t} - \hat{\tau}) - \theta_1 + \phi) \quad (30)$$

$$\frac{dR_2}{d\hat{t}} = \hat{N}_2 R_2 + \eta R_1 (\hat{t} - \hat{\tau}) \cos(\theta_1 (\hat{t} - \hat{\tau}) - \theta_2 + \phi) \quad (31)$$

$$\frac{d\theta_1}{d\hat{t}} = -\alpha \hat{N}_1 + \eta \frac{R_2 (\hat{t} - \hat{\tau})}{R_1} \sin(\theta_2 (\hat{t} - \hat{\tau}) - \theta_1 + \phi) \quad (32)$$

$$\frac{d\theta_2}{d\hat{t}} = -\alpha \hat{N}_2 + \eta \frac{R_1 (\hat{t} - \hat{\tau})}{R_2} \sin(\theta_1 (\hat{t} - \hat{\tau}) - \theta_2 + \phi). \quad (33)$$

This model is simplified by only considering instantaneous coupling where $\hat{\tau} = 0$. The slowly varying electric field phase difference,

$$\Theta = \theta_2 - \theta_1, \quad (34)$$

is now introduced to reduce the system of six equations to a system of five equations as shown in the following equations:

$$\frac{dR_1}{d\hat{t}} = \hat{N}_1 R_1 + \eta R_2 \cos(\Theta + \phi) \quad (35)$$

$$\frac{dR_2}{d\hat{t}} = \hat{N}_2 R_2 + \eta R_1 \cos(\Theta - \phi) \quad (36)$$

$$\frac{d\Theta}{d\hat{t}} = -\alpha (\hat{N}_2 - \hat{N}_1) - \eta \left(\frac{R_1}{R_2} \sin(\Theta - \phi) + \frac{R_2}{R_1} \sin(\Theta + \phi) \right) \quad (37)$$

$$T \frac{d\hat{N}_1}{d\hat{t}} = \hat{P}_1 - \hat{N}_1 - (1 + 2\hat{N}_1) R_1^2 \quad (38)$$

$$T \frac{d\hat{N}_2}{d\hat{t}} = \hat{P}_2 - \hat{N}_2 - (1 + 2\hat{N}_2) R_2^2. \quad (39)$$

Table 3 shows some approximate values of the parameters in Equations (35-39). This system of equations along with the appropriate computational methods are used to investigate the modulation response of evanescently coupled twin diode lasers and mutually coupled twin diode lasers, but an investigation of the modulation response of a solitary laser is provided in the next section to establish a performance baseline and to define some terms.

Table 3. Typical values of the parameters in Equations (35-39).

Symbol	Typical Value	Reference
α	≈ 5	[1][6][15][22]
η	$\approx 10^{-2}$	[22]
T	$\approx 10^3$	[1][6][22]
\hat{P}	≈ 1	[1][6][22]

2.3 Modulation Response of a Solitary Diode Laser

Following the procedure found in Reference [14] and [21], The rate equations derived in Section 2.2 are used to model a solitary diode laser and solve for its infinitesimal modulation response. This lays out a performance baseline for the twin optically coupled diode laser system, defines some terms and outlines the basic procedure for the linear stability analysis that will be used to analyze the coupled laser system.

The solitary laser is modeled by taking $\eta = 0$ in Equations (35-39) and choosing one set of subscripts to arrive at

$$\frac{dR}{d\hat{t}} = \hat{N}R \quad (40)$$

$$\frac{d\theta}{d\hat{t}} = -\alpha\hat{N} \quad (41)$$

$$T\frac{d\hat{N}}{d\hat{t}} = \hat{P} - \hat{N} - (1 + 2\hat{N})R^2. \quad (42)$$

To find the infinitesimal modulation response Equations (40-42) are linearized about their steady state values. The steady state values are found by equating $\frac{dR}{d\hat{t}}$ in Equation (40) to zero. This means that either $R = 0$ or $\hat{N} = 0$. Since $R \neq 0$, otherwise the laser is off, then $\hat{N} = 0$, which means the laser is operating at threshold. This result is then substituted into Equation (41) and Equation (42) to find the steady

state values of R and θ . The steady state solutions are

$$\hat{N}_s = 0 \quad (43)$$

$$R_s = \sqrt{\hat{P}_s}, \quad (44)$$

where \hat{N}_s is the steady state dimensionless excess carrier density, R_s is the steady state dimensionless slowly varying electric field amplitude, and \hat{P}_s is the steady state dimensionless excess electrical pumping rate. The steady state slowly varying electric field phase (θ_s) becomes an arbitrary constant. The linearization is accomplished by substituting

$$R(\hat{t}) = R_s + \delta R(\hat{t}) \quad (45)$$

$$\theta(\hat{t}) = \theta_s + \delta\theta(\hat{t}) \quad (46)$$

$$\hat{N}(\hat{t}) = \hat{N}_s + \delta\hat{N}(\hat{t}) \quad (47)$$

$$\hat{P}(\hat{t}) = \hat{P}_s + \delta\hat{P}(\hat{t}) \quad (48)$$

into Equations (40-42). The equations are then expanded while eliminating terms such as δR^2 and $\delta R\delta\hat{N}$ since the δ terms are defined as small oscillations about the steady state values. The results of this linearization are

$$\frac{d}{dt}\delta R = \sqrt{\hat{P}_s}\delta\hat{N} \quad (49)$$

$$\frac{d}{dt}\delta\theta = -\alpha\delta\hat{N} \quad (50)$$

$$T\frac{d}{dt}\delta\hat{N} = -(1 + 2\hat{P}_s)\delta\hat{N} - 2\sqrt{\hat{P}_s}\delta R + \delta\hat{P}. \quad (51)$$

This set of equations can also be written in matrix form,

$$\frac{d}{dt} \begin{bmatrix} \delta R \\ \delta\theta \\ \delta\hat{N} \end{bmatrix} = \begin{bmatrix} 0 & 0 & \sqrt{\hat{P}_s} \\ 0 & 0 & -\alpha \\ -2\sqrt{\hat{P}_s}/T & 0 & -(1 + 2\hat{P}_s)/T \end{bmatrix} \begin{bmatrix} \delta R \\ \delta\theta \\ \delta\hat{N} \end{bmatrix} + \begin{bmatrix} 0 \\ 0 \\ 1/T \end{bmatrix} \delta\hat{P}, \quad (52)$$

where the 3x3 matrix is the Jacobian of Equations (40-42) when the dimensionless excess electrical pumping rate is held constant. The dynamics of this system will now be examined with no modulation signal, $\delta\hat{P} = 0$, in order to define some terms that will be used throughout this document.

Taking $\delta\hat{P} = 0$, Differentiating Equation (51) and substituting Equation (49) for $\frac{d}{dt}\delta R$ gives a second order ordinary differential equation.

$$\delta\hat{N}'' + \frac{1 + 2\hat{P}_s}{T}\delta\hat{N}' + \frac{2\hat{P}_s}{T}\delta\hat{N} = 0. \quad (53)$$

The solution of Equation (53) is

$$\delta\hat{N}(t) = C_1 e^{\lambda_+ t} + C_2 e^{\lambda_- t}, \quad (54)$$

where

$$\lambda_+ = -\left(\frac{1 + 2\hat{P}_s}{2T}\right) + i\sqrt{\frac{2\hat{P}_s}{T} - \left(\frac{1 + 2\hat{P}_s}{2T}\right)^2}$$

$$\lambda_- = -\left(\frac{1 + 2\hat{P}_s}{2T}\right) - i\sqrt{\frac{2\hat{P}_s}{T} - \left(\frac{1 + 2\hat{P}_s}{2T}\right)^2}$$

are the eigenvalues of the Jacobian matrix in Equation (52) and C_n are arbitrary constants. This solution is a damped simple harmonic oscillator with a dimensionless relaxation damping coefficient,

$$\gamma_r \equiv \frac{1 + 2\hat{P}_s}{2T}, \quad (55)$$

and a dimensionless relaxation oscillation frequency,

$$\omega_r \equiv \sqrt{\frac{2\hat{P}_s}{T} - \gamma_r^2}. \quad (56)$$

This oscillation frequency is approximated as

$$\omega_r \approx \sqrt{\frac{2\hat{P}_s}{T}}, \quad (57)$$

since T is approximately 10^3 making $2\hat{P}_s/T \gg \gamma_r^2$. The approximate form of the dimensionless relaxation oscillation frequency in Equation (57) will be used when referring to this frequency. These terms can now be used in the derivation of the infinitesimal modulation response as well as in subsequent equations in this document.

The infinitesimal modulation response is found by taking the Fourier transform of Equations (49,53) as shown in the following equations:

$$i\omega_m \mathcal{F}\{\delta R\} = \sqrt{\hat{P}_s} \mathcal{F}\{\delta \hat{N}\} \quad (58)$$

$$\frac{i\omega_m}{T} \mathcal{F}\{\delta \hat{P}\} = -\omega_m^2 \mathcal{F}\{\delta \hat{N}\} + 2\gamma_r i\omega_m \mathcal{F}\{\delta \hat{N}\} + \omega_r^2 \mathcal{F}\{\delta \hat{N}\}, \quad (59)$$

where $\mathcal{F}\{\}$ indicates a Fourier transform operation and ω_m is the dimensionless angular modulation frequency. Equations (58,59) are now solved for the Fourier transform of the electric field divided by the Fourier transform of the carrier density to arrive at

$$\frac{\mathcal{F}\{\delta R\}}{\mathcal{F}\{\delta \hat{P}\}} = \frac{\sqrt{\hat{P}_s}}{T(\omega_r^2 - \omega_m^2 + 2i\gamma_r\omega_m)}. \quad (60)$$

Taking the absolute value yields

$$\left| \frac{\mathcal{F}\{\delta R\}}{\mathcal{F}\{\delta \hat{P}\}} \right| = \frac{\sqrt{\hat{P}_s}}{T\sqrt{(\omega_m^2 - \omega_r^2)^2 + 4\gamma_r^2\omega_m^2}}. \quad (61)$$

Finally, Equation (61) is normalized to the response at zero frequency to arrive at

$$M(\omega_m) = \frac{\omega_r^2}{\sqrt{(\omega_m^2 - \omega_r^2)^2 + 4\gamma_r^2\omega_m^2}}, \quad (62)$$

where M denotes the modulation response.

The infinitesimal modulation response is also found by using the matrix form of the linearized equations. This treatment is the basis for calculating the infinitesimal modulation response of the coupled system. The first step is taking the Fourier transform of Equation (52) to arrive at

$$i\omega_m \begin{bmatrix} \mathcal{F}\{\delta R\} \\ \mathcal{F}\{\delta\theta\} \\ \mathcal{F}\{\delta\hat{N}\} \end{bmatrix} = J \begin{bmatrix} \mathcal{F}\{\delta R\} \\ \mathcal{F}\{\delta\theta\} \\ \mathcal{F}\{\delta\hat{N}\} \end{bmatrix} + \begin{bmatrix} 0 \\ 0 \\ 1/T \end{bmatrix} \mathcal{F}\{\delta\hat{P}\}, \quad (63)$$

where J is the Jacobian matrix. Collecting like terms and dividing by the Fourier transform of the electrical pumping rate modulation yields

$$\begin{bmatrix} \frac{\mathcal{F}\{\delta R\}}{\mathcal{F}\{\delta\hat{P}\}} \\ \frac{\mathcal{F}\{\delta\theta\}}{\mathcal{F}\{\delta\hat{P}\}} \\ \frac{\mathcal{F}\{\delta\hat{N}\}}{\mathcal{F}\{\delta\hat{P}\}} \end{bmatrix} = [J - i\omega_m I]^{-1} \begin{bmatrix} 0 \\ 0 \\ -\frac{1}{T} \end{bmatrix}, \quad (64)$$

where I is the identity matrix. Finally, the modulation response is found by multiplying the first row third column of the matrix in Equation (64) by $-\frac{1}{T}$, taking the absolute value, and normalizing to the response at a modulation frequency of zero.

$$M(\omega_m) = \left| \frac{[J - i\omega_m I]_{1,3}^{-1}}{J_{1,3}^{-1}} \right|. \quad (65)$$

Since J is known analytically, Equation (65) can be put into the same form as Equation (62).

Equations (55,56,62) show that the infinitesimal modulation response of a solitary laser is externally manipulated by adjusting the dimensionless excess electrical pumping rate. Using the parameters in Table 1, Figure 4 shows the infinitesimal modulation response of a solitary laser at various steady state operating currents. The function has a Lorentzian shape with a peak around the relaxation oscillation frequency. The trend in the figures is that increased electrical pumping rates increase

the relaxation oscillation and bandwidth, but do little to flatten the modulation response.

The methods outlined in this section for the solitary laser will now be used in the model for twin optically coupled diode lasers to develop the computational methods in Chapter III. The same linear stability analysis, outlined in this section, will be applied in Section 3.1 to determine the stability of the steady states for the coupled system. This will lead into Section 3.2 where the method for computing the infinitesimal modulation response of the coupled system is derived. This computational method will mirror the matrix treatment of the solitary laser. Finally, a numerical method will be employed in Section 3.3 to calculate the nonlinear modulation response.

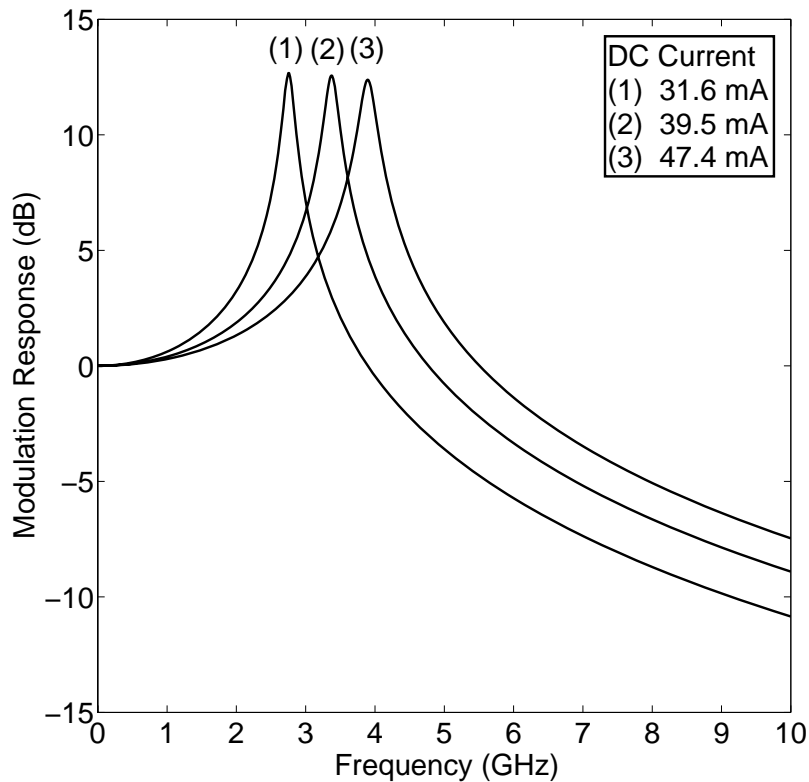


Figure 4. Modulation response of a solitary InGaAsP diode laser at an operating current of (a) 31.6 mA, (b) 39.5 mA, and (c) 47.4 mA. The bandwidths at +6 dB are 2.4 GHz, 2.9 GHz, and 3.4 GHz respectively. Increasing current increases bandwidth but does little to suppress the resonance at the relaxation oscillation frequency.

III. Computational Methods

In order to compute the modulation response of the coupled system, three computational methods are developed. Since the diode lasers are modulated about a set of steady states, the stability of the steady states needs to be determined through a linear stability analysis. This is accomplished by looking at small perturbations about the steady states. If these perturbations grow, then the steady states are unstable and not appropriate for modulation. Using concepts from the linear stability analysis, the infinitesimal modulation response is calculated. This computation produces results whether the steady states are stable or not and can be used to explore the parameter space. The final computational method calculates the modulation response by numerically integrating the rate equations and taking Fourier transforms. This method is used to examine the modulation response at modulation amplitudes beyond the infinitesimal limit, but requires stable steady states.

3.1 Linear Stability Analysis

The stability of the steady states is determined by examining the effect of small perturbations about the steady states. This is accomplished through a linearization of the rate equations by substituting

$$R_1(\hat{t}) = R_{s,1} + \delta R_1(\hat{t}) \quad (66)$$

$$R_2(\hat{t}) = R_{s,2} + \delta R_2(\hat{t}) \quad (67)$$

$$\Theta(\hat{t}) = \Theta_s + \delta\Theta(\hat{t}) \quad (68)$$

$$\hat{N}_1(\hat{t}) = \hat{N}_{s,1} + \delta\hat{N}_1(\hat{t}) \quad (69)$$

$$\hat{N}_2(\hat{t}) = \hat{N}_{s,2} + \delta\hat{N}_2(\hat{t}) \quad (70)$$

into Equations (35-39) while taking \hat{P}_1 and \hat{P}_2 as constants and ignoring products of delta terms. As with the case of the solitary laser in Section 2.3, the result is

expressed using the Jacobian matrix of the system as shown in the following:

$$\frac{d}{d\hat{t}} \begin{bmatrix} \delta R_1 \\ \delta R_2 \\ \delta \Theta \\ \delta \hat{N}_1 \\ \delta \hat{N}_2 \end{bmatrix} = J \begin{bmatrix} \delta R_1 \\ \delta R_2 \\ \delta \Theta \\ \delta \hat{N}_1 \\ \delta \hat{N}_2 \end{bmatrix}. \quad (71)$$

Solutions to Equation (71) are exponential functions,

$$\begin{aligned} \delta R_1(\hat{t}) &= C_{1,1}e^{\lambda_1\hat{t}} + C_{1,2}e^{\lambda_2\hat{t}} + C_{1,3}e^{\lambda_3\hat{t}} + C_{1,4}e^{\lambda_4\hat{t}} + C_{1,5}e^{\lambda_5\hat{t}} \\ \delta R_2(\hat{t}) &= C_{2,1}e^{\lambda_1\hat{t}} + C_{2,2}e^{\lambda_2\hat{t}} + C_{2,3}e^{\lambda_3\hat{t}} + C_{2,4}e^{\lambda_4\hat{t}} + C_{2,5}e^{\lambda_5\hat{t}} \\ \delta \Theta(\hat{t}) &= C_{3,1}e^{\lambda_1\hat{t}} + C_{3,2}e^{\lambda_2\hat{t}} + C_{3,3}e^{\lambda_3\hat{t}} + C_{3,4}e^{\lambda_4\hat{t}} + C_{3,5}e^{\lambda_5\hat{t}} \\ \delta \hat{N}_1(\hat{t}) &= C_{4,1}e^{\lambda_1\hat{t}} + C_{4,2}e^{\lambda_2\hat{t}} + C_{4,3}e^{\lambda_3\hat{t}} + C_{4,4}e^{\lambda_4\hat{t}} + C_{4,5}e^{\lambda_5\hat{t}} \\ \delta \hat{N}_2(\hat{t}) &= C_{5,1}e^{\lambda_1\hat{t}} + C_{5,2}e^{\lambda_2\hat{t}} + C_{5,3}e^{\lambda_3\hat{t}} + C_{5,4}e^{\lambda_4\hat{t}} + C_{5,5}e^{\lambda_5\hat{t}}, \end{aligned} \quad (72)$$

where λ_i are eigenvalues of the Jacobian matrix and $C_{m,n}$ are arbitrary constants. For the system to be stable, the real part of all eigenvalues must be less than or equal to zero. If the real part of any eigenvalue is greater than zero then there will be a term that will grow exponentially, thus destabilizing the system.

3.2 Infinitesimal Modulation Response

The stability of the steady states is determined by examining small perturbations about the steady states, which can also be used to calculate the infinitesimal modulation response. The infinitesimal modulation response is calculated by including small perturbations in the excess electrical pumping rate along with perturbations in the steady states. This is accomplished by adding another vector to Equation(71)

to arrive at

$$\frac{d}{dt} \begin{bmatrix} \delta R_1 \\ \delta R_2 \\ \delta \Theta \\ \delta \hat{N}_1 \\ \delta \hat{N}_2 \end{bmatrix} = J \begin{bmatrix} \delta R_1 \\ \delta R_2 \\ \delta \Theta \\ \delta \hat{N}_1 \\ \delta \hat{N}_2 \end{bmatrix} + \delta \hat{P} \begin{bmatrix} 0 \\ 0 \\ 0 \\ \frac{1}{T} \\ \frac{L}{T} \end{bmatrix}, \quad (73)$$

where $\delta \hat{P}$ is an infinitesimal modulation about the steady state excess electrical pumping rate. For simplicity and practicality, the lasers are modulated with the same signal ($\delta \hat{P}$) except for the ability to modulate the signal out-of-phase which is controlled by the term L [1; 6]. This term takes the value of 1 for in-phase modulation and -1 for out-of-phase modulation. The next step is to take the Fourier transform of Equation (73) and collect terms to arrive at

$$-\mathcal{F}\{\delta \hat{P}\} \begin{bmatrix} 0 \\ 0 \\ 0 \\ \frac{1}{T} \\ \frac{L}{T} \end{bmatrix} = [J - i\omega_m I] \begin{bmatrix} \mathcal{F}\{\delta R_1\} \\ \mathcal{F}\{\delta R_2\} \\ \mathcal{F}\{\delta \Theta\} \\ \mathcal{F}\{\delta \hat{N}_1\} \\ \mathcal{F}\{\delta \hat{N}_2\} \end{bmatrix}. \quad (74)$$

Now, Equation (74) is divided by $\mathcal{F}\{\delta \hat{P}\}$ and multiplied by $(J - i\omega I)^{-1}$ to produce

$$\begin{bmatrix} \frac{\mathcal{F}\{\delta R_1\}}{\mathcal{F}\{\delta \hat{P}\}} \\ \frac{\mathcal{F}\{\delta R_2\}}{\mathcal{F}\{\delta \hat{P}\}} \\ \frac{\mathcal{F}\{\delta \Theta\}}{\mathcal{F}\{\delta \hat{P}\}} \\ \frac{\mathcal{F}\{\delta \hat{N}_1\}}{\mathcal{F}\{\delta \hat{P}\}} \\ \frac{\mathcal{F}\{\delta \hat{N}_2\}}{\mathcal{F}\{\delta \hat{P}\}} \end{bmatrix} = -[J - i\omega_m I]^{-1} \begin{bmatrix} 0 \\ 0 \\ 0 \\ \frac{1}{T} \\ \frac{L}{T} \end{bmatrix}. \quad (75)$$

From Equation (75) the infinitesimal modulation response for each laser is extracted.

$$M_1(\omega_m) = \frac{|H_{1,4} + LH_{1,5}|}{|J_{1,4}^{-1} + LJ_{1,5}^{-1}|} \quad (76)$$

$$M_2(\omega_m) = \frac{|H_{2,4} + LH_{2,5}|}{|J_{2,4}^{-1} + LJ_{2,5}^{-1}|} \quad (77)$$

where

$$H = [J - i\omega I]^{-1}.$$

The *Matlab*[®] code that implements this algorithm is included in Appendix C. As long as a set of steady states can be found, this algorithm can be used to find the infinitesimal modulation response of a twin diode laser system whether the steady states are stable or unstable. The infinitesimal modulation response provides some information about the response of the system, but does not provide information about how the system behaves when the modulation is not infinitesimal.

A numerical algorithm is developed in the next section to calculate the non-linear modulation response. This will be used to confirm the results of the infinitesimal modulation response as well as provide a tool that can be used to examine the modulation response when the modulation amplitude of the electrical pumping rate is not infinitesimal.

3.3 *Non-linear Modulation Response*

The modulation response is calculated numerically by first integrating the rate equations for a period of time with a sinusoidal modulation added to the steady state dimensionless excess electrical pumping rate. With this data, the discrete Fourier transform of the slowly varying electric field amplitude and the discrete Fourier transform of the excess electrical pumping rate are calculated, but only at the frequency of the sinusoidal modulation. This is because the Fourier transform of the electrical pumping rate will be a single spike at the modulation frequency. Essentially, the

sinusoidal modulation is sampling the modulation response at one modulation frequency. After the Fourier transforms, The absolute value of each Fourier transform element is taken and the appropriate ratio is made. This process is then repeated for other modulation frequencies as desired. The C++ source code for the program which implements this algorithm is included in Appendix D.

The program starts by reading an input file which includes information such as laser parameters, coupling parameters, modulation frequency points, stable steady states and variables to control simulation times. After reading the input file, the integration is completed using a fourth order Runge-Kutta algorithm [24] with initial values at the steady states and with a sinusoidal modulation added to the steady state excess electrical pumping rate. The Runge-Kutta algorithm is

$$\begin{aligned}
R_1[n] &= R_1[n-1] + (K_{1,1} + 2K_{2,1} + 2K_{3,1} + K_{4,1})/6 \\
R_2[n] &= R_2[n-1] + (K_{1,2} + 2K_{2,2} + 2K_{3,2} + K_{4,2})/6 \\
\Theta[n] &= \Theta[n-1] + (K_{1,3} + 2K_{2,3} + 2K_{3,3} + K_{4,3})/6 \\
\hat{N}_1[n] &= \hat{N}_1[n-1] + (K_{1,4} + 2K_{2,4} + 2K_{3,4} + K_{4,4})/6 \\
\hat{N}_2[n] &= \hat{N}_2[n-1] + (K_{1,5} + 2K_{2,5} + 2K_{3,5} + K_{4,5})/6
\end{aligned} \tag{78}$$

where

$$\begin{aligned}
K_{1,m} &= \hat{dt} f_m(\hat{t}, R_1[n-1], R_2[n-1], \Theta[n-1], \hat{N}_1[n-1], \hat{N}_2[n-1]) \\
K_{2,m} &= \hat{dt} f_m(\hat{t} + \frac{\hat{dt}}{2}, R_1[n-1] + \frac{K_{1,1}}{2}, R_2[n-1] + \frac{K_{1,2}}{2}, \Theta[n-1] + \frac{K_{1,3}}{2}, \dots \\
&\quad \hat{N}_1[n-1] + \frac{K_{1,4}}{2}, \hat{N}_2[n-1] + \frac{K_{1,5}}{2}) \\
K_{3,m} &= \hat{dt} f_m(\hat{t} + \frac{\hat{dt}}{2}, R_1[n-1] + \frac{K_{2,1}}{2}, R_2[n-1] + \frac{K_{2,2}}{2}, \Theta[n-1] + \frac{K_{2,3}}{2}, \dots \\
&\quad \hat{N}_1[n-1] + \frac{K_{2,4}}{2}, \hat{N}_2[n-1] + \frac{K_{2,5}}{2}) \\
K_{4,m} &= \hat{dt} f_m(\hat{t} + \hat{dt}, R_1[n-1] + K_{3,1}, R_2[n-1] + K_{3,2}, \Theta[n-1] + K_{3,3}, \dots \\
&\quad \hat{N}_1[n-1] + K_{3,4}, \hat{N}_2[n-1] + K_{3,5})
\end{aligned}$$

and

$$f_1 = \frac{dR_1}{dt}; \quad f_2 = \frac{dR_2}{dt}; \quad f_3 = \frac{d\Theta}{dt}; \quad f_4 = \frac{d\hat{N}_1}{dt}; \quad f_5 = \frac{d\hat{N}_2}{dt}.$$

To make the discrete Fourier transform element easier to calculate and to ensure that the modulation frequency appears at one of the discrete frequency points, the integration time is set to a specified number of modulation periods. This also ensures that the Fourier element of interest is at the same number of frequency points from zero no matter what the value of the modulation frequency. Once integration is complete, the discrete Fourier transform element is calculated for the slowly varying electric field amplitudes out of each laser diode and for the excess electrical pumping rate. The Fourier element is calculated using

$$F(p+1) = \sum_{l=1}^N f(l) \cos(2\pi p(l-1)/N) - i \sum_{l=1}^N f(l) \sin(2\pi p(l-1)/N), \quad (79)$$

where $F(p+1)$ is the Fourier component, N is the total number of simulation points, f is the array that contains the simulation data in the time domain, l is the array index, and p is the number of modulation periods. Once the Fourier elements are calculated, the absolute values of electric field amplitude Fourier elements are divided by the absolute value of the electrical pumping rate Fourier element. Finally, the results are converted to decibels and printed to the output file. This algorithm calculates the non-normalized value of the modulation response at one frequency, so the process is repeated for additional modulation frequencies. Outside of the program, the results are normalized to the value of the infinitesimal modulation response at zero frequency.

IV. Simulations

In this chapter two coupling schemes are investigated. The first is mutual coupling, shown in Figure 2(a), where photons are exchanged through the direct injection of photons through the output couplers [8; 17]. The second is evanescent coupling, shown in Figure 2(b), where photons are exchanged through the evanescent waves that penetrate the waveguides created by the active regions [1; 6; 7; 9; 18; 19].

4.1 Mutual Coupling

This section investigates injection coupling as shown in Figure 2(b) where the insulating layer may be a very small air gap. For this system a coupling phase of zero is used in Equations (35-39), giving

$$\frac{dR_1}{dt} = \hat{N}_1 R_1 + \eta R_2 \cos(\Theta) \quad (80)$$

$$\frac{dR_2}{dt} = \hat{N}_2 R_2 + \eta R_1 \cos(\Theta) \quad (81)$$

$$\frac{d\Theta}{dt} = -\alpha(\hat{N}_2 - \hat{N}_1) - \eta \sin(\Theta) \left(\frac{R_1}{R_2} + \frac{R_2}{R_1} \right) \quad (82)$$

$$T \frac{d\hat{N}_1}{dt} = \hat{P}_1 - \hat{N}_1 - (1 + 2\hat{N}_1) R_1^2 \quad (83)$$

$$T \frac{d\hat{N}_2}{dt} = \hat{P}_2 - \hat{N}_2 - (1 + 2\hat{N}_2) R_2^2. \quad (84)$$

Depending on the insulating material the coupling phase may not be zero, but a coupling phase of zero was chosen for ease of computing the steady states. For simplicity the steady states for Equations (80-84) are calculated with symmetric steady state excess electrical pumping rates ($\hat{P}_{s,1} = \hat{P}_{s,2}$). It is shown in Appendix A that the only stable steady states are

$$\Theta_s = 0, \quad \hat{N}_s = -\eta, \quad R_s = \sqrt{\frac{\hat{P}_s + \eta}{1 - 2\eta}}, \quad (85)$$

where

$$\hat{N}_s = \hat{N}_{s,1} = \hat{N}_{s,2}, \quad R_s = R_{s,1} = R_{s,2}.$$

Figure 5 shows regions of stability for a typical parameter space.

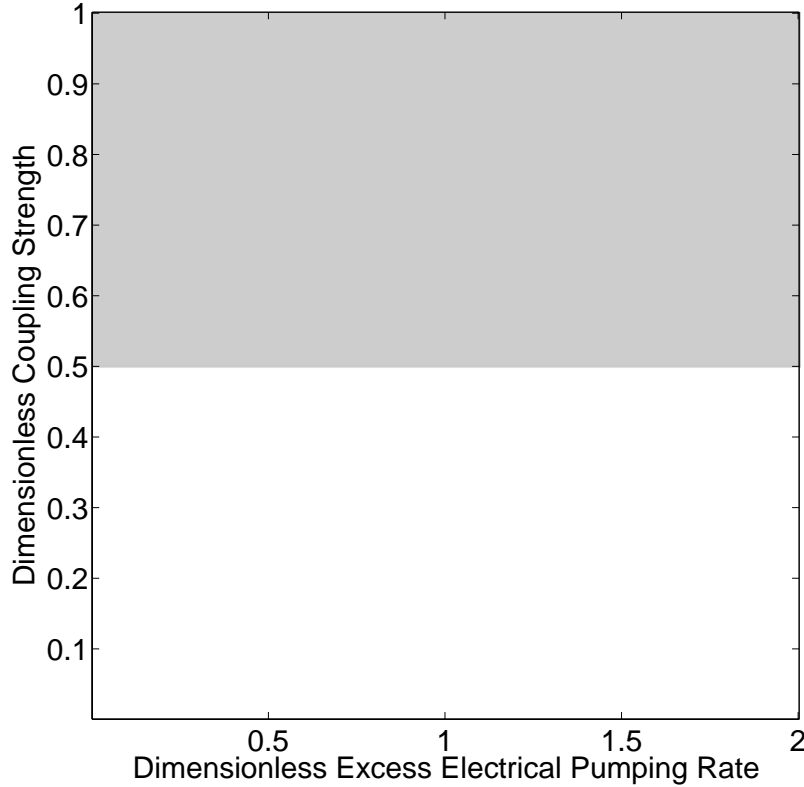


Figure 5. Regions of stability for symmetric steady states of mutual coupling with symmetric pumping rates and a steady state phase difference of zero.

For a system of twin InGaAsP lasers at a normalized coupling strength of 0.1 and a steady state current of 47.4 mA ($\hat{P}_s \approx 1$), the modulation response shown in Figure 6 has a +6 dB bandwidth of about 3.5 GHz for in-phase modulation and a -6 dB bandwidth of about 4.4 GHz for out-of-phase modulation. Figure 6(a) shows that increased coupling for in-phase modulation slightly increased bandwidth as well as the position of the peak response. Figure 6(b) shows that increased coupling for out-of-phase modulation increases bandwidth by suppressing the resonance at the frequency of relaxation oscillations.

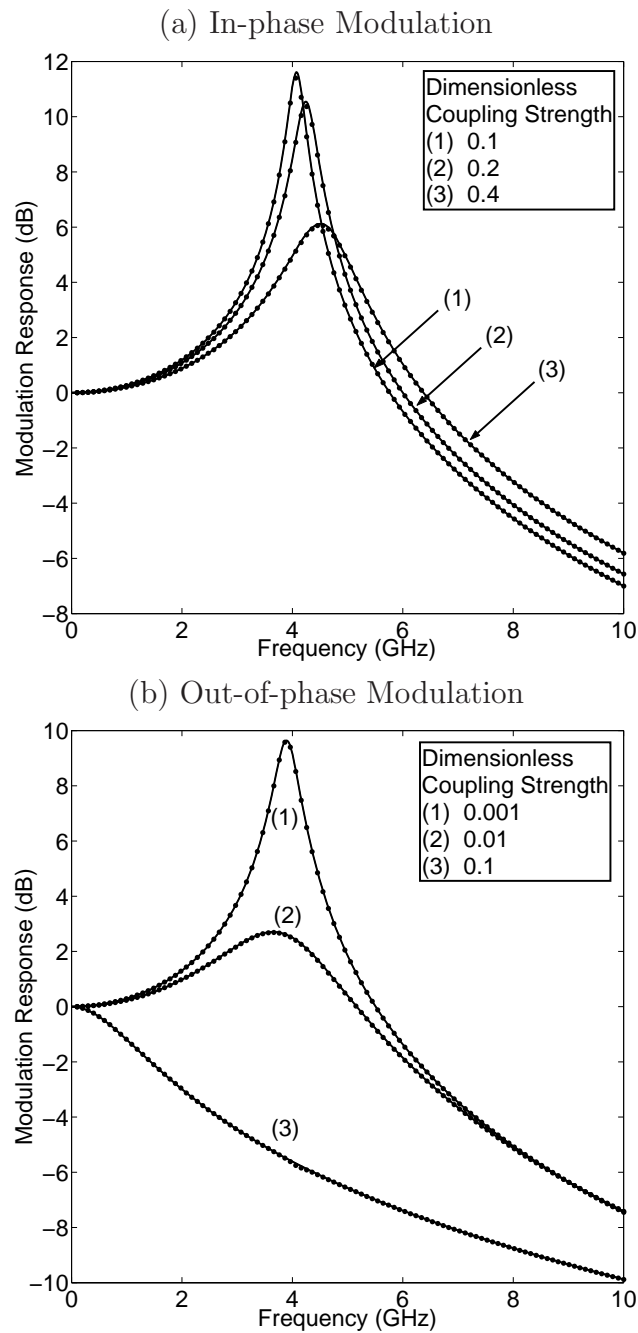


Figure 6. (a) Modulation response of twin mutually coupled diode lasers with in-phase modulation (b) Modulation response of twin mutually coupled diode lasers with out-of-phase modulation. The steady state current is held at 47.4 mA. Solid lines are the infinitesimal modulation limit and dots are numerical results attained by modulating the current at an amplitude of $316 \mu\text{A}$.

4.2 Evanescent Coupling

A system of twin evanescently coupled diode lasers as shown in Figure 2b is modeled by using a coupling phase of $\frac{\pi}{2}$ in Equations (35-39) [1; 6].

$$\frac{dR_1}{dt} = \hat{N}_1 R_1 - \eta R_2 \sin(\Theta) \quad (86)$$

$$\frac{dR_2}{dt} = \hat{N}_2 R_2 + \eta R_1 \sin(\Theta) \quad (87)$$

$$\frac{d\Theta}{dt} = -\alpha(\hat{N}_2 - \hat{N}_1) + \eta \cos(\Theta) \left(\frac{R_1}{R_2} - \frac{R_2}{R_1} \right) \quad (88)$$

$$T \frac{d\hat{N}_1}{dt} = \hat{P}_1 - \hat{N}_1 - (1 + 2\hat{N}_1) R_1^2 \quad (89)$$

$$T \frac{d\hat{N}_2}{dt} = \hat{P}_2 - \hat{N}_2 - (1 + 2\hat{N}_2) R_2^2. \quad (90)$$

Modeling the laser system using Equations (86-90) is discussed in References [1; 6; 18]. It is shown in Reference [1] and Reference [6] that the laser system can possibly be effectively modulated beyond the relaxation oscillation frequency by modulating the lasers out-of-phase. A figure similar to Figure 7a is presented in Reference [1] and [6] showing the effects of modulating the diode lasers out-of-phase. The eigenvalues of the Jacobian indicate that there are two resonances. One resonance is around the frequency of relaxation oscillations at about 3.9 GHz and the other is at about 20.5 GHz. The figure shows that the bandwidth is improved by about five times, but the steady states about which the system is modulated are unstable. This means that the response may never be observed. Appendix B shows the solution for the steady states when the steady state excess electrical pumping rates are equated ($\hat{P}_{s,1} = \hat{P}_{s,2}$). The only real-valued stable steady states are

$$\Theta_s = 0 \quad \hat{N}_s = 0 \quad R_s = \sqrt{\hat{P}_s} \quad (91)$$

$$\Theta_s = \pi \quad \hat{N}_s = 0 \quad R_s = \sqrt{\hat{P}_s}, \quad (92)$$

where

$$\hat{N}_s = \hat{N}_{s,1} = \hat{N}_{s,2}, \quad R_s = R_{s,1} = R_{s,2},$$

but as previously indicated they are unstable over a large region of the typical parameter space as shown in Figure 8. It appears that the states are stable when coupling strength is very low or when coupling strength is very high and the lasers are held close to threshold. In the first case, the lasers are essentially operating as solitary lasers. For the second case, running the lasers close to threshold is impractical and does not fit well with the model. This instability problem is remedied in the next sections by introducing asymmetric pumping rates or gain saturation into the model.

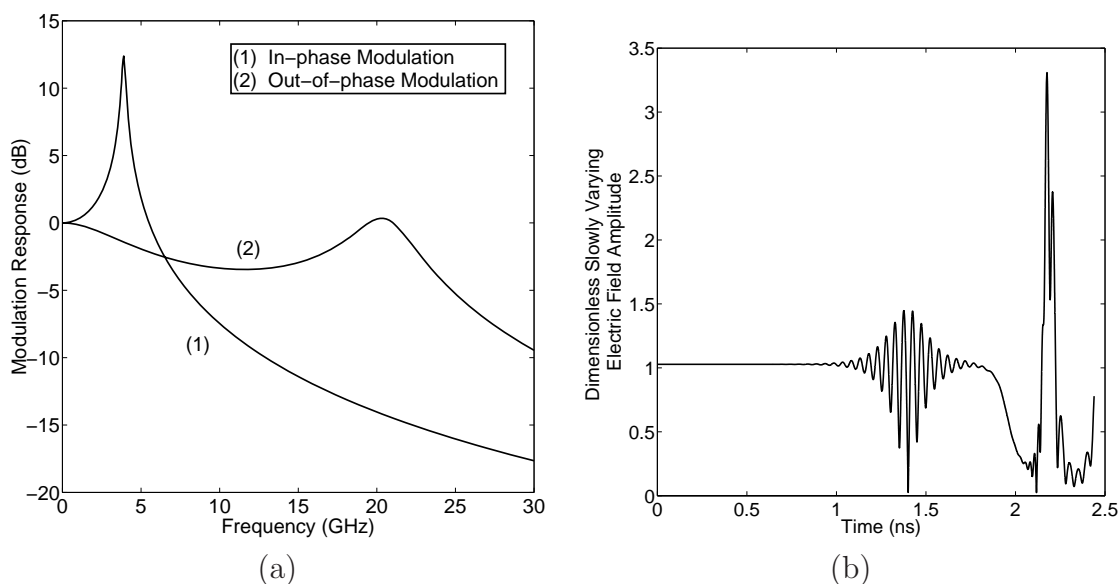


Figure 7. (a) Modulation response of twin evanescently coupled InGaAsP diode lasers. The steady state phase difference is π , current through the lasers is 47.4 mA, and dimensionless coupling strength is 0.1. The steady states are unstable with the secondary resonance growing exponentially at a rate of approximately 10^{10}s^{-1} . (b) The time evolution of the dimensionless slowly varying electric field in one of the lasers with unstable steady states that are computed to within 10^{-6} and no modulation. The electric field starts at the steady state value, but begins to oscillate at the secondary resonance frequency of 20.5 GHz and then begins to oscillate chaotically.

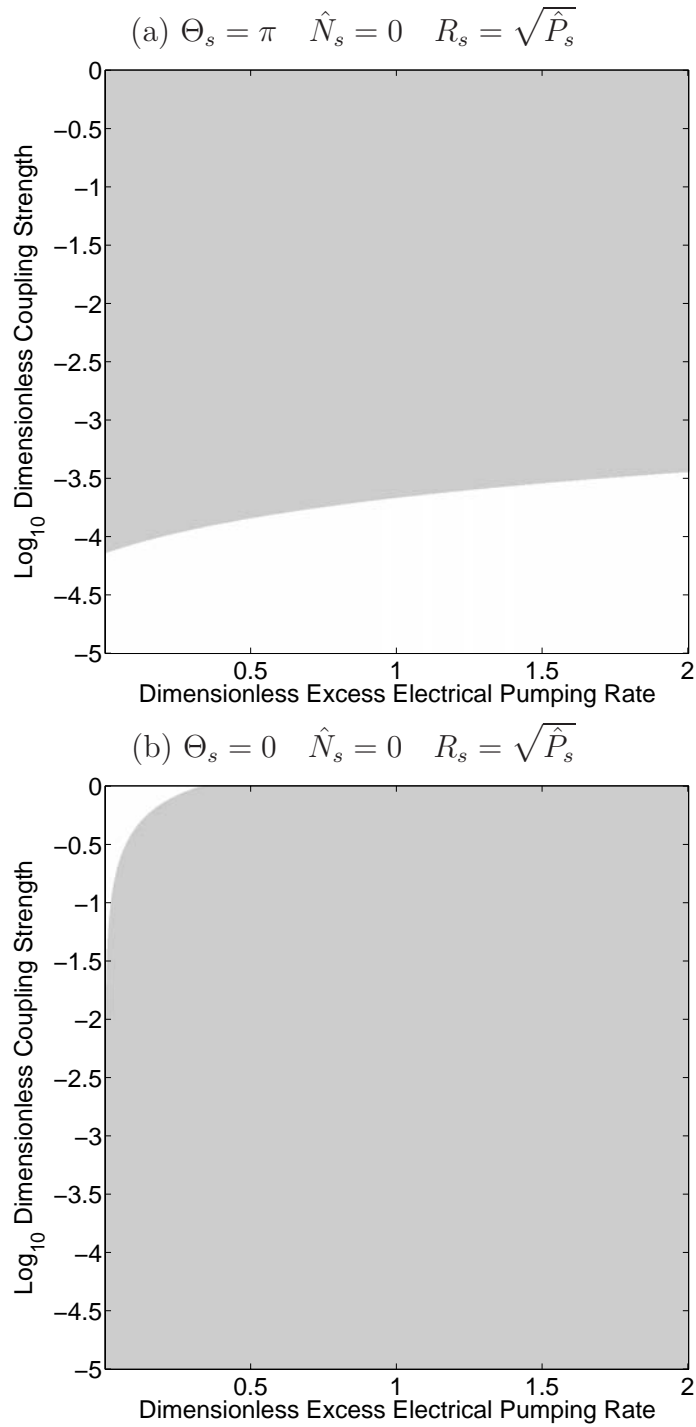


Figure 8. Regions of stability for symmetric steady states of evanescent coupling with symmetric pumping rates and a steady state phase difference of (a) π and (b) 0. Regions in gray are where the steady states are unstable. Regions in white are regions where the steady states are stable.

4.2.1 *Asymmetric Pumping Stabilization.* For a typical InGaAsP laser the symmetric steady states with symmetric excess electrical pumping rates are unstable for a coupling strength of 0.1 and a synchronous steady state electrical current of 47.4 mA (Figure 7). One way of remedying this is by making the DC currents through the lasers asymmetric. Asymmetric steady states with asymmetric excess electrical pumping rates are found numerically using Newton's method [24]. For this algorithm the steady state excess electrical pumping rates are defined as

$$\hat{P}_{s,2} = \hat{P}_s + \Delta \quad (93)$$

$$\hat{P}_{s,1} = \hat{P}_s - \Delta, \quad (94)$$

where Δ is defined as the dimensionless excess electrical pumping rate displacement. Substituting Equations (93, 94) into Equations (35-39) yields a new set of rate equations.

$$\frac{dR_1}{d\hat{t}} = \hat{N}_1 R_1 + \eta R_2 \cos(\Theta + \phi) \quad (95)$$

$$\frac{dR_2}{d\hat{t}} = \hat{N}_2 R_2 + \eta R_1 \cos(\Theta - \phi) \quad (96)$$

$$\frac{d\Theta}{d\hat{t}} = -\alpha(\hat{N}_2 - \hat{N}_1) - \eta \left(\frac{R_1}{R_2} \sin(\Theta - \phi) + \frac{R_2}{R_1} \sin(\Theta + \phi) \right) \quad (97)$$

$$T \frac{d\hat{N}_1}{d\hat{t}} = \hat{P}_s - \Delta - \hat{N}_1 - (1 + 2\hat{N}_1) R_1^2 \quad (98)$$

$$T \frac{d\hat{N}_2}{d\hat{t}} = \hat{P}_s + \Delta - \hat{N}_2 - (1 + 2\hat{N}_2) R_2^2. \quad (99)$$

The term \hat{P}_s is used to calculate the symmetric steady states in Equations (91,92), which are then used as the initial guess in a Newton's method algorithm [24]. A first order correction to the initial guess is made by calculating the inverse of the Jacobian matrix and multiplying it by the rate equations evaluated at the initial conditions. This correction is then subtracted from the initial guess. This process is repeated with the new steady state values until the steady states are reached, the maximum number of iterations is exceeded or a tolerance (Equation (101)) is met. This algorithm is

shown in Equation (100), and the *Matlab*[®] function which implements it is included in Appendix E.

$$\vec{x}_{n+1} = \vec{x}_n - J_n^{-1} \vec{f}(\vec{x}_n), \quad (100)$$

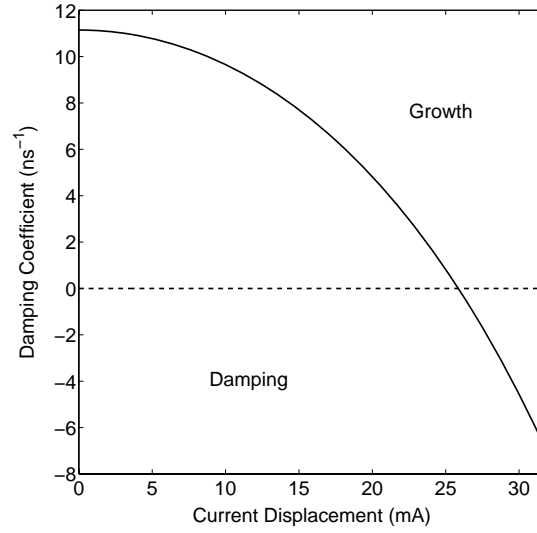
where

$$\vec{x} = \begin{bmatrix} R_{s,1} \\ R_{s,2} \\ \Theta_s \\ \hat{N}_{s,1} \\ \hat{N}_{s,2} \end{bmatrix}, \quad J = \begin{bmatrix} \left. \frac{\partial \vec{f}}{\partial R_1} \right|_{\vec{x}} & \left. \frac{\partial \vec{f}}{\partial R_2} \right|_{\vec{x}} & \left. \frac{\partial \vec{f}}{\partial \Theta} \right|_{\vec{x}} & \left. \frac{\partial \vec{f}}{\partial \hat{N}_1} \right|_{\vec{x}} & \left. \frac{\partial \vec{f}}{\partial \hat{N}_2} \right|_{\vec{x}} \end{bmatrix}, \quad \vec{f} = \begin{bmatrix} \frac{dR_1}{dt} \\ \frac{dR_2}{dt} \\ \frac{d\Theta}{dt} \\ \frac{d\hat{N}_1}{dt} \\ \frac{d\hat{N}_2}{dt} \end{bmatrix},$$

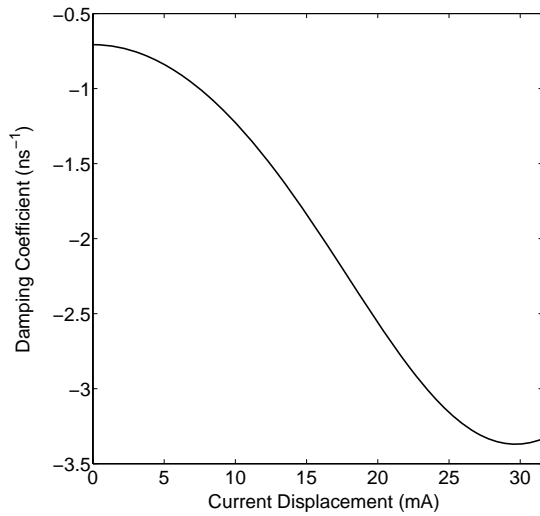
and

$$\text{Tol} > J_n^{-1} \vec{f}(\vec{x}_n) \bullet J_n^{-1} \vec{f}(\vec{x}_n). \quad (101)$$

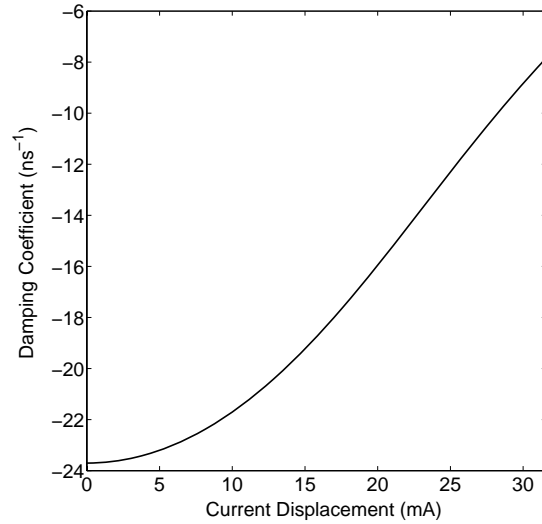
By increasing the steady state electrical pumping rate displacement (Δ), a set of stable steady states is attained as shown in Figure 9(a). Figure 10 is created using the same parameters as used to create Figure 7, but with a current displacement of 28.4 mA. Since the system is no longer symmetric, the modulation response out of each laser is different. Figure 10 shows that both in-phase and out-of-phase modulation result in a +6 dB bandwidth of about 4 GHz. Due to the secondary resonance the out-of-phase response has an additional band that spans about 19.4 GHz from about 4.7 GHz to about 24.1 GHz. This is a significant improvement in bandwidth, but the different responses out of each laser may not be desirable in a practical twin laser diode system. Stabilization through gain saturation may be a more practical avenue for stability and is addressed in the next section.



(a)



(b)



(c)

Figure 9. Damping coefficients vs. current displacement. The steady states become stable at about 25 mA of current displacement where the coefficient in (a) becomes negative.

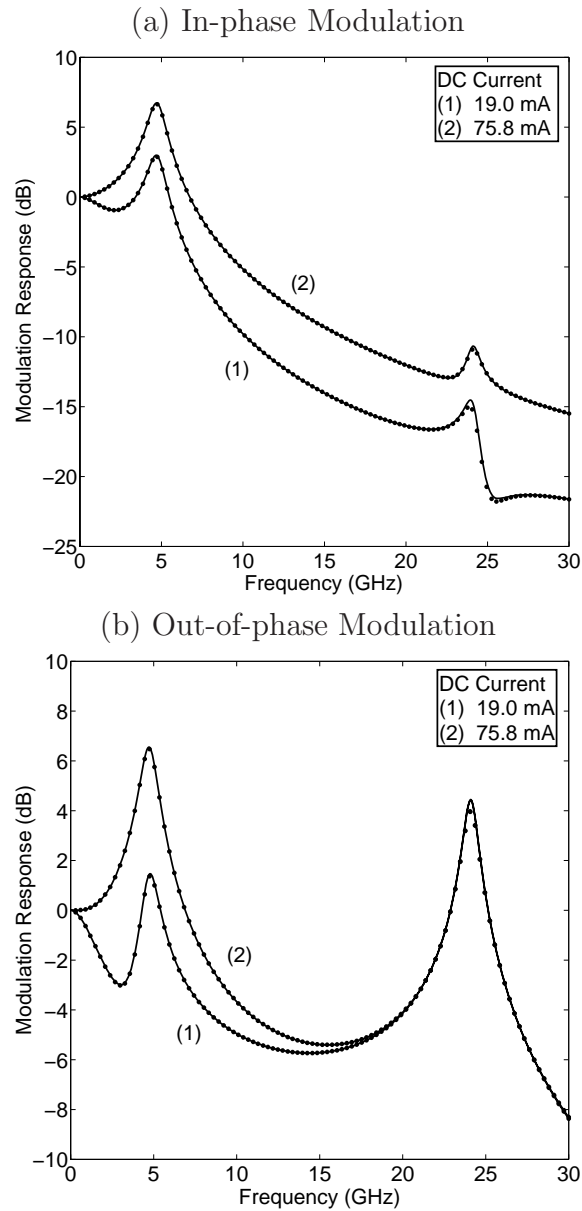


Figure 10. Modulation response for (a) in-phase and (b) out-of-phase modulation of a typical InGaAsP diode laser. Solid lines are the infinitesimal modulation limit and dots are numerical results attained by modulating at an amplitude of $316 \mu\text{A}$. The current displacement is 28.4 mA , the dimensionless coupling strength is 0.1 , and the phase difference is π . The response for in-phase modulation has a $+6 \text{ dB}$ bandwidth of about 4.3 GHz . The response for out-of-phase modulation has a $+6 \text{ dB}$ bandwidth of about 4.4 GHz , but there is another band that spans 19.4 GHz from the relaxation oscillation frequency of 4.7 GHz to the secondary resonance frequency of 24.1 GHz .

4.2.2 *Gain Saturation Stabilization.* Nichols and Winful [19] show that gain saturation stabilizes the symmetric steady states shown in Equation (92). Figure 11 illustrates this finding. In order to take advantage of this effect, a phenomenological two-level saturable gain model is used [19].

$$G(N, E) = \frac{1/\tau_p + G_N(N - N_{th})}{1 + \beta|E|^2} \quad (102)$$

where β is the gain saturation coefficient. Equation (102) replaces the linear gain model in Equation (3). The rate equations are normalized using the same variables as shown in Equations (21) with the addition of the dimensionless gain saturation coefficient ($\hat{\beta}$).

$$\hat{\beta} = \frac{2\beta}{G_N\tau_c}. \quad (103)$$

Typical values of the gain saturation coefficient are 10^{-17} cm^3 for InGaAsP [19] making typical values for the dimensionless gain saturation coefficient around 0.01. Including the saturable gain model, decomposing, and normalizing yields

$$\frac{dR_1}{d\hat{t}} = \frac{1}{2} \left(\frac{1 + 2\hat{N}_1}{1 + \hat{\beta}R_1^2} - 1 \right) R_1 + \eta R_2 \cos(\Theta + \phi) \quad (104)$$

$$\frac{dR_2}{d\hat{t}} = \frac{1}{2} \left(\frac{1 + 2\hat{N}_2}{1 + \hat{\beta}R_2^2} - 1 \right) R_2 + \eta R_1 \cos(\Theta - \phi) \quad (105)$$

$$\frac{d\Theta}{d\hat{t}} = -\alpha \left(\frac{1 + 2\hat{N}_2}{1 + \hat{\beta}R_2^2} - \frac{1 + 2\hat{N}_1}{1 + \hat{\beta}R_1^2} \right) - \eta \left(\frac{R_1}{R_2} \sin(\Theta - \phi) + \frac{R_2}{R_1} \sin(\Theta + \phi) \right) \quad (106)$$

$$T \frac{d\hat{N}_1}{d\hat{t}} = \hat{P}_1 - \hat{N}_1 - \left(\frac{1 + 2\hat{N}_1}{1 + \hat{\beta}R_1^2} \right) R_1^2 \quad (107)$$

$$T \frac{d\hat{N}_2}{d\hat{t}} = \hat{P}_2 - \hat{N}_2 - \left(\frac{1 + 2\hat{N}_2}{1 + \hat{\beta}R_2^2} \right) R_2^2. \quad (108)$$

The symmetric steady states with symmetric excess electrical pumping rates are found to be

$$\Theta_s = 0 \quad \hat{N}_s = \frac{\hat{\beta}\hat{P}_s + 2\eta}{2 + \hat{\beta}} \quad R_s = \sqrt{\frac{\hat{P}_s - \hat{N}_s}{1 + 2\hat{N}_s - \hat{\beta}(\hat{P}_s - \hat{N}_s)}} \quad (109)$$

$$\Theta_s = \pi \quad \hat{N}_s = \frac{\hat{\beta}\hat{P}_s - 2\eta}{2 + \hat{\beta}} \quad R_s = \sqrt{\frac{\hat{P}_s - \hat{N}_s}{1 + 2\hat{N}_s - \hat{\beta}(\hat{P}_s - \hat{N}_s)}}. \quad (110)$$

By increasing the value of $\hat{\beta}$, a set of stable steady states is attained at a value of about 0.02 as shown in Figure 12. A gain saturation coefficient of 0.03 was chosen to calculate the modulation response shown in Figure 13. The in-phase modulation response has a -6 dB bandwidth of about 8.2 GHz and peaks around the relaxation oscillation frequency at 3.5 GHz. The out-of-phase modulation has a -6 dB bandwidth of about 9.9 GHz from the origin, but has an additional -6 dB band with a width of about 10.5 GHz from 19.8 GHz to about 30.3 GHz. The out-of-phase modulation peaks around the secondary resonance frequency of 26.6 GHz. Comparing Figure 7 and Figure 13 shows that a higher gain saturation coefficient preserves the basic features of the modulation response when the gain is linear. Higher gain saturation seems to dampen the resonance at the relaxation oscillation frequency while enhancing the resonance at the secondary resonance frequency. This stabilization scheme also does not create two different modulation responses for each laser as was seen in the asymmetric stabilization scheme.

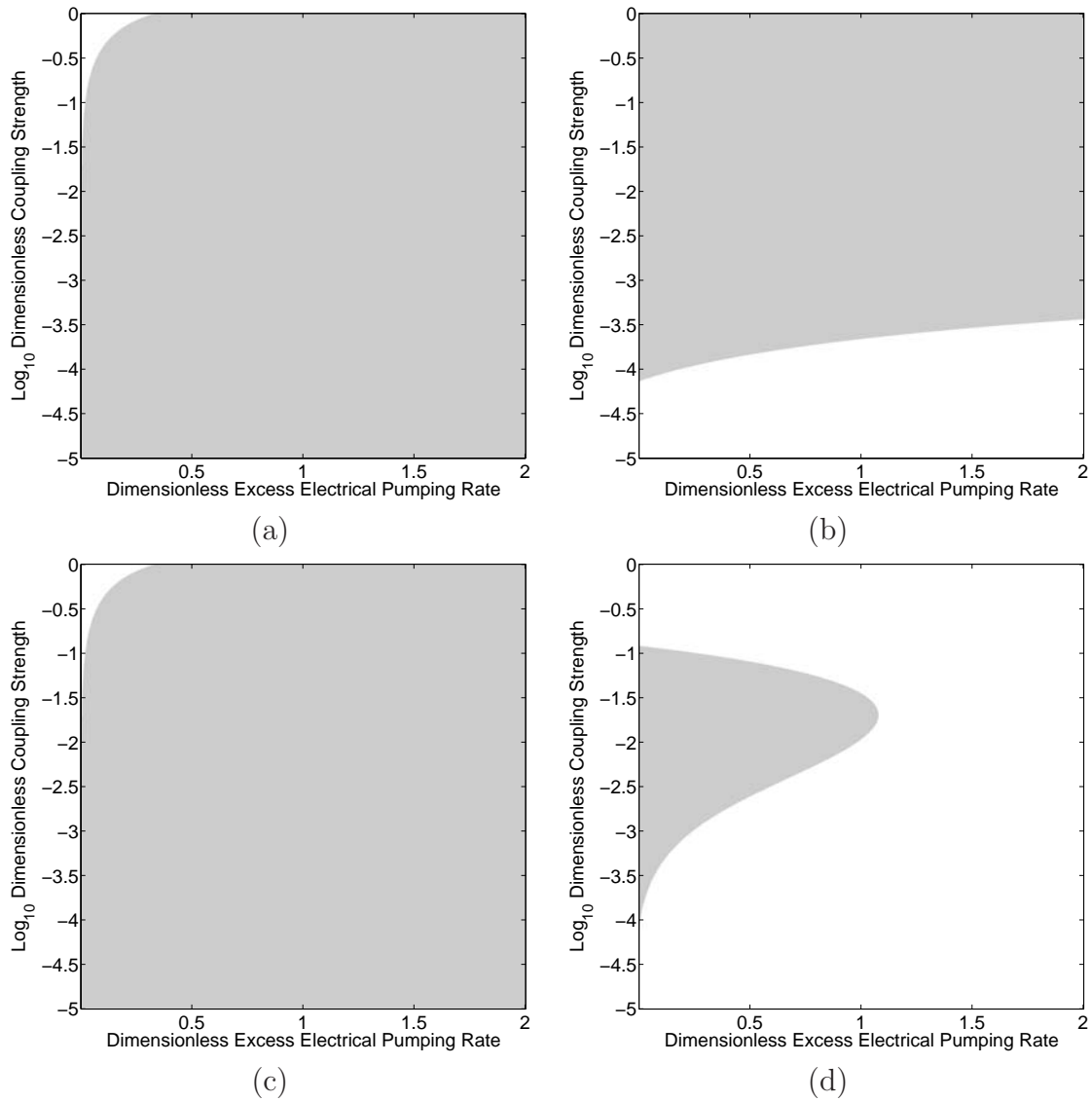
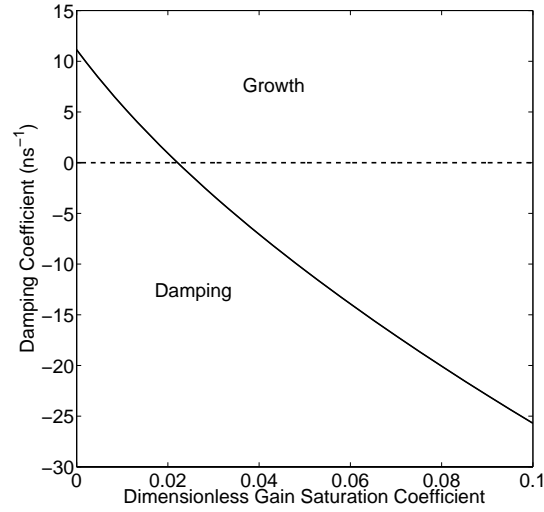
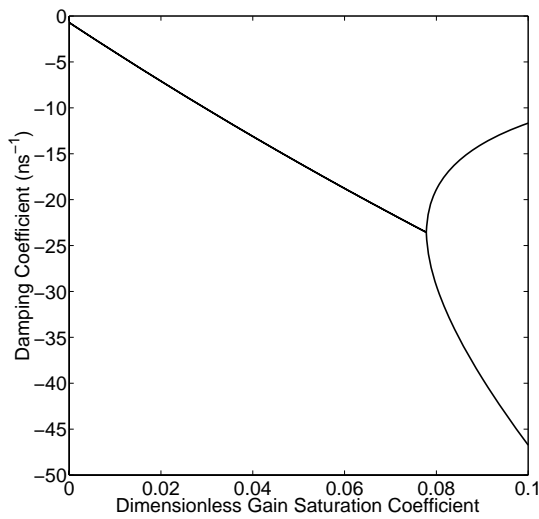


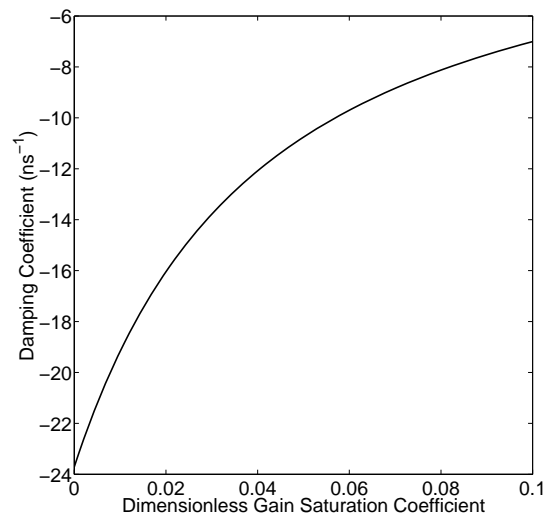
Figure 11. Regions of stability for symmetric steady states of evanescent coupling with symmetric pumping rates. (a) Steady state phase is zero and gain saturation is ignored. (b) Steady state phase is π and gain saturation is ignored. (c) Steady state phase is zero with gain saturation. (d) Steady state phase is π with gain saturation. Regions in gray are where the steady states are unstable. Regions in white are regions where the steady states are stable.



(a)



(b)



(c)

Figure 12. Damping coefficients vs. dimensionless gain saturation coefficient. The steady states become stable at a coefficient value of about 0.02 where the coefficient in (a) becomes negative. The split in (b) is due to the associated resonance frequency becoming imaginary.

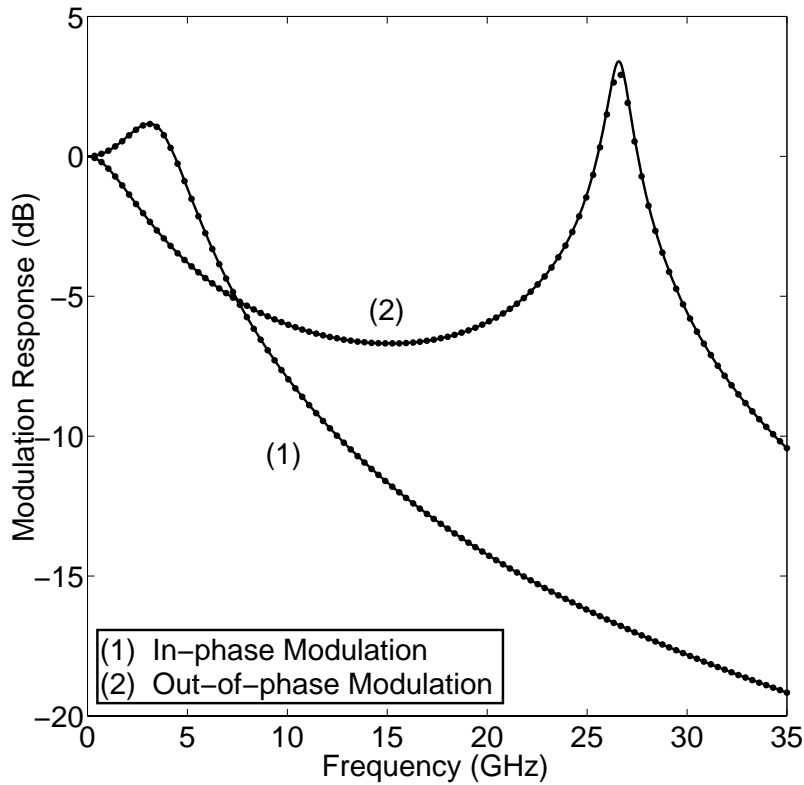


Figure 13. Modulation response of twin evanescently coupled InGaAsP diode lasers. Solid lines are the infinitesimal modulation limit and dots are numerical results attained by modulating at an amplitude of $316 \mu\text{A}$. The steady state phase difference is π , current through the lasers is 47.4 mA , dimensionless coupling strength is 0.1 , and dimensionless gain coefficient is 0.03 . (a) The response for in-phase modulation peaks at the free running relaxation oscillation frequency of 3.5 GHz and has a -6 dB bandwidth of about 8.2 GHz . (b) The response for out-of-phase modulation peaks at the secondary resonance frequency of 26.6 GHz and has a -6 dB bandwidth of about 9.9 GHz , but the secondary resonance creates another -6 dB band from about 19.8 GHz to about 30.3 GHz .

V. Summary and Conclusions

Laser rate equations for electric field, and carrier density can be used to study the modulation response of a system of twin optically coupled diode lasers. The synchronous steady states can be calculated analytically and used in a numerical algorithm to calculate steady states where the normalized excess electrical pumping rates in each laser are not the same. The stability of the steady states can be examined using a linear stability analysis that makes use of the Jacobian of the rate equations. An algorithm using concepts from the linear stability analysis can be used to calculate the infinitesimal modulation response. In addition to the infinitesimal modulation response, the non-linear modulation response can be calculated by using a numerical method which integrates the rate equations, takes Fourier transforms, and makes the appropriate ratios. For mutually coupled lasers, it is shown that the modulation bandwidth of the coupled lasers does not show significant improvement over the modulation bandwidth of the solitary laser, but the resonance at the frequency of free running relaxation oscillations is suppressed while the coupled lasers are modulated out-of-phase allowing for a flatter response. References [1] and [6] state that the modulation bandwidth for evanescently coupled diode lasers is significantly larger than the bandwidth for a solitary diode laser when modulating the signals out-of-phase, but the steady states about which the lasers are modulated are unstable. It is shown in this document and Reference [18] that the steady states are unstable over most of the parameter space. This is remedied by introducing asymmetric steady state currents through the laser or by introducing saturable gain [19]. Making use of this, the benefits of twin evanescently coupled diode lasers as reported in References [1] and [6] can be realized. Simulations in this document show that asymmetric stabilization allows the coupled system to be effectively modulated out to about 25 GHz with a +6 dB band from 0-4.3 GHz and a -6 dB band spanning 19.4 GHz from 4.7-24.1 GHz. For gain saturation stabilization, simulations show that the coupled system can be effectively modulated out to a frequency of about 25 GHz with a -6 dB band from 0-9.9 GHz and another -6 dB band spanning 19.8 GHz from 10.5-30.3 GHz.

There are some additional analytic, experimental, and modeling projects that can grow from this work. Analytic expressions can be derived for most of the steady states and infinitesimal modulation responses that were calculated using the algorithms in Appendix E and Appendix C, but will require significant simplifications and approximations to make them useful. Additional work can include experiments where the modulation response is calculated for evanescent coupling [7] or for mutual coupling [8] and compared to the results of the model. Additional modeling can be completed by investigating different coupling schemes such as changing coupling phases for mutual coupling and alternate configurations such as ring lasers [25]. In this work the numerical calculation of the modulation response was used as a confirmation of the infinitesimal modulation response, but can be used to investigate the non-linear dynamics of the system. One example of this is the investigation of sub-harmonic and super-harmonic resonances [26] that occur when the modulation amplitude is not infinitesimal as shown in Figure 14.

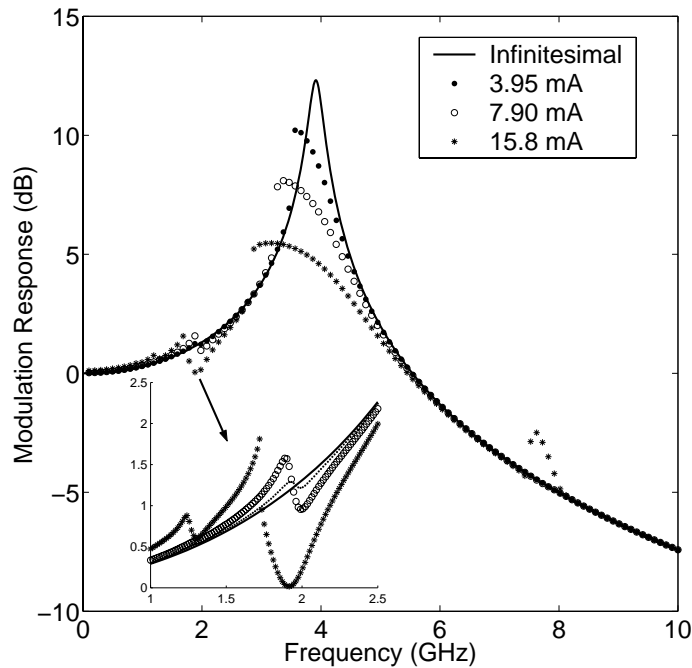


Figure 14. Non-linear modulation response of twin mutually coupled InGaAsP diode lasers with in-phase modulation. Coupling strength is 0.001 and the steady state current is held at 47.4 mA. The legend indicates the modulation amplitude of the current.

This work has implications in current communications technology and future technologies such as chaotic communications and photonic devices. Diode lasers are currently used in today's communications systems, but there is always room for improvement. Increases in bandwidth and improved modulation properties, realized through coupled diode laser systems, can make current systems faster and more efficient. It was shown that the steady states can be unstable for optically coupled diode lasers, but this may not be an unwelcome circumstance. These states could possibly be used to place the system into a chaotic state which can then be used to encrypt information. Finally, this work can be used to drive upcoming technologies in optoelectronic devices and photonic integrated circuitry, which can lead to the next generation of communications and computing devices.

Appendix A. Steady States for Mutual Coupling

The steady states of Equations (80-84) where $\hat{P}_{s,2} = \hat{P}_{s,1} = \hat{P}_s$ are solved by satisfying

$$0 = \hat{N}_{s,1}R_{s,1} + \eta R_{s,2} \cos(\Theta_s) \quad (111)$$

$$0 = \hat{N}_{s,2}R_{s,2} + \eta R_{s,1} \cos(\Theta_s) \quad (112)$$

$$0 = -\alpha(\hat{N}_{s,2} - \hat{N}_{s,1}) - \eta \sin(\Theta_s) \left(\frac{R_{s,1}}{R_{s,2}} + \frac{R_{s,2}}{R_{s,1}} \right) \quad (113)$$

$$0 = \hat{P}_s - \hat{N}_{s,1} - (1 + 2\hat{N}_{s,1})R_{s,1}^2 \quad (114)$$

$$0 = \hat{P}_s - \hat{N}_{s,2} - (1 + 2\hat{N}_{s,2})R_{s,2}^2. \quad (115)$$

These equations are solved for the steady states by reducing the equations to a system of two equations with the steady state dimensionless excess carrier densities as the variables. After this is accomplished, the new system is solved for the steady state carrier densities. The first step is to solve Equation (111) for $\hat{N}_{s,1}$, Equation (112) for $\hat{N}_{s,2}$, Equation (114) for $R_{s,1}$ and Equation (115) for $R_{s,2}$. This result in

$$\hat{N}_{s,1} = -\eta \frac{R_{s,2}}{R_{s,1}} \cos(\Theta_s) \quad (116)$$

$$\hat{N}_{s,2} = -\eta \frac{R_{s,1}}{R_{s,2}} \cos(\Theta_s) \quad (117)$$

$$R_{s,1} = \sqrt{\frac{\hat{P}_s - \hat{N}_{s,1}}{1 + 2\hat{N}_{s,1}}} \quad (118)$$

$$R_{s,2} = \sqrt{\frac{\hat{P}_s - \hat{N}_{s,2}}{1 + 2\hat{N}_{s,2}}}. \quad (119)$$

These equations show the steady state carrier densities as functions of steady state amplitudes and the steady state amplitudes as functions of steady state carrier densities. The phase dependence is eliminated by dividing Equation (116) by Equation (117) to arrive at

$$\frac{\hat{N}_{s,1}}{\hat{N}_{s,2}} = \frac{R_{s,2}^2}{R_{s,1}^2} \quad (120)$$

The first equation that relates $\hat{N}_{s,1}$ to $\hat{N}_{s,2}$ is found by substituting Equations (118, 119) into Equation (120) to arrive at

$$\hat{P}_s(\hat{N}_{s,2} - \hat{N}_{s,1}) - (\hat{N}_{s,2}^2 - \hat{N}_{s,1}^2) - 2\hat{N}_{s,2}\hat{N}_{s,1}(\hat{N}_{s,2} - \hat{N}_{s,1}) = 0. \quad (121)$$

In order to find another relation between $\hat{N}_{s,1}$ and $\hat{N}_{s,2}$, the trigonometric identity,

$$\sin^2(\Theta_s) + \cos^2(\Theta_s) = 1, \quad (122)$$

is used. The $\sin^2(\Theta_s)$ is found by solving either Equation (116) or Equation (117) for $\sin(\Theta_s)$, squaring the result, and including Equation (120) where appropriate. The $\cos^2(\Theta_s)$ is found by solving Equation(113) for $\cos(\Theta_s)$, squaring the result, and including Equation (120) where appropriate. The results of this are

$$\sin^2(\Theta_s) = \frac{\alpha^2(\hat{N}_{s,2} - \hat{N}_{s,1})^2}{\eta^2\left(\frac{\hat{N}_{s,2}}{\hat{N}_{s,1}} + \frac{\hat{N}_{s,1}}{\hat{N}_{s,2}} + 2\right)} \quad (123)$$

$$\cos^2(\Theta_s) = \frac{\hat{N}_{s,1}\hat{N}_{s,2}}{\eta^2}. \quad (124)$$

Using Equation (122) and Equations (123,124) a second relation between $\hat{N}_{s,1}$ and $\hat{N}_{s,2}$ is found to be

$$\hat{N}_{s,2}\hat{N}_{s,1} \left((\hat{N}_{s,2} + \hat{N}_{s,1})^2 + \alpha^2(\hat{N}_{s,2} - \hat{N}_{s,1})^2 \right) - \eta^2(\hat{N}_{s,2} + \hat{N}_{s,1})^2 = 0. \quad (125)$$

Equations (121, 125) are now solved for the steady state carrier densities. For simplicity

$$y = \hat{N}_{s,2} + \hat{N}_{s,1} \quad (126)$$

$$x = \hat{N}_{s,2} - \hat{N}_{s,1} \quad (127)$$

are substituted into Equations (121,125) to arrive at

$$0 = \hat{P}_s x - (y^2 - x^2)\left(\frac{x}{2}\right) - xy \quad (128)$$

$$0 = \frac{y^2 - x^2}{4}(y^2 + \alpha^2 x^2) - \eta^2 y^2. \quad (129)$$

Equation (128) is now solved for x .

$$x = \begin{cases} 0 \\ \pm \sqrt{y^2 + 2y - 2\hat{P}_s}. \end{cases} \quad (130)$$

The solution where $x = 0$ is substituted into Equation (129) to yield the symmetric steady states. These steady states are

$$\Theta_s = 0 \quad \hat{N}_s = -\eta \quad R_s = \sqrt{\frac{\hat{P}_s + \eta}{1 - 2\eta}} \quad (131)$$

$$\Theta_s = \pi \quad \hat{N}_s = \eta \quad R_s = \sqrt{\frac{\hat{P}_s - \eta}{1 + 2\eta}}, \quad (132)$$

where

$$\hat{N}_s = \hat{N}_{s,1} = \hat{N}_{s,2}, \quad R_s = R_{s,1} = R_{s,2}.$$

The linear stability analysis in Section 3.1 is used to determine if the steady states are stable with the parameters in Table 1, a steady state excess electrical pumping rate from zero to two and a dimensionless coupling strength from zero to one. The results of this analysis are shown in Figure 15. Either of the remaining solutions can

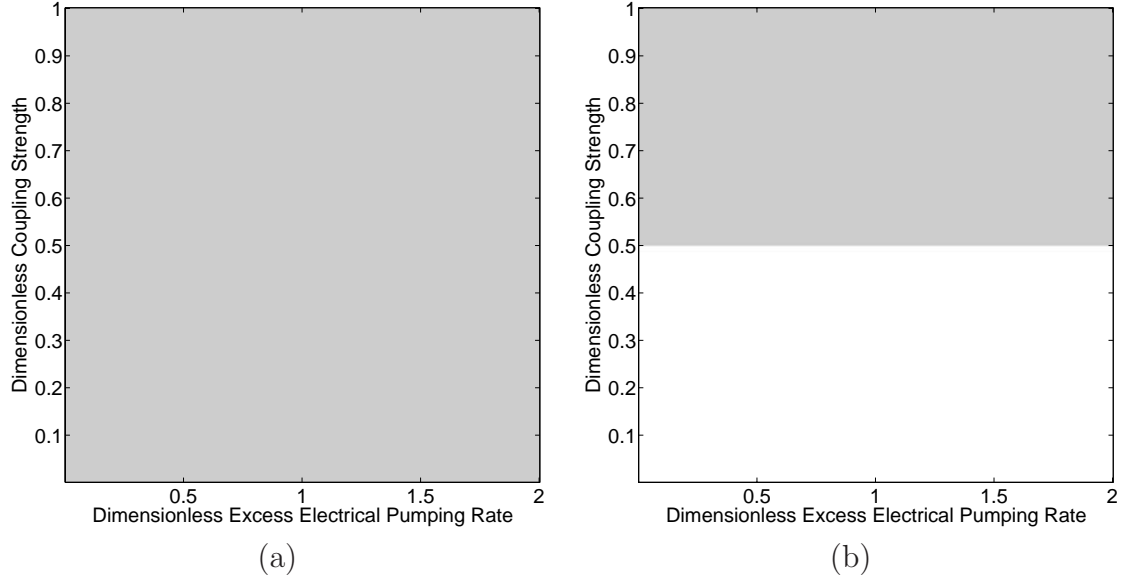


Figure 15. Regions of stability for symmetric steady states of mutual coupling with symmetric pumping rates and a steady state phase difference of (a) π and (b) 0. Regions in gray are where the steady states are unstable. Regions in white are regions where the steady states are stable.

be substituted into Equation (129) to find

$$\begin{aligned}
0 &= y^3 (1 + \alpha^2) \\
&+ y^2 \left(2(\alpha^2 + \eta^2) - \hat{P}_s(1 + \alpha^2) \right) \\
&- y \left(4\hat{P}_s\alpha^2 \right) \\
&+ \left(2\hat{P}_s^2\alpha^2 \right).
\end{aligned} \tag{133}$$

The asymmetric steady states are found by solving Equation (133) using the cubic formula found in most algebra references. After solving for y , the solutions are substituted into

$$\hat{N}_{s,1} = \frac{1}{2} \left(y \pm \sqrt{y^2 + 2y - 2\hat{P}_s} \right) \tag{134}$$

$$\hat{N}_{s,2} = \frac{1}{2} \left(y \mp \sqrt{y^2 + 2y - 2\hat{P}_s} \right). \tag{135}$$

to find the steady state carrier densities which are then used to solve for the steady state amplitudes and steady state phase difference. For these steady states to be valid, they must be real and stable. For the steady states to be real, y must be real as well as a part of the space $((y \leq -1 - \sqrt{1 + 2\hat{P}_s}) \cup (y \geq -1 + \sqrt{1 + 2\hat{P}_s}))$ to satisfy Equation (130). With this and the linear stability analysis, the steady states either do not exist or are unstable for the parameters in Table 1, a steady state excess electrical pumping rate from zero to two and a dimensionless coupling strength from zero to one. The results of this analysis are shown in Figure 16.

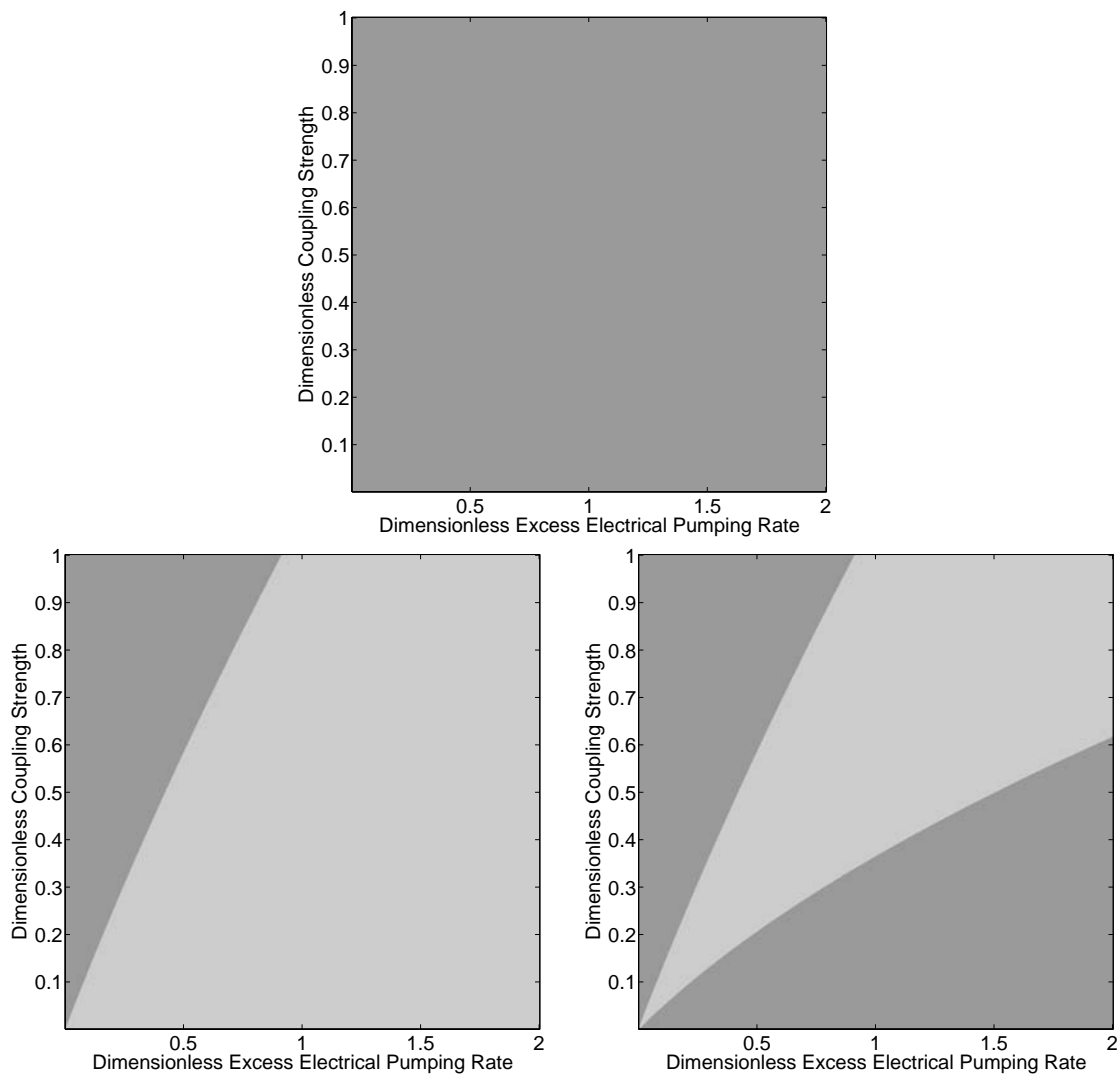


Figure 16. Regions of stability and existence for asymmetric steady states of mutual coupling with symmetric pumping rates. Regions in gray are where the steady states are unstable. Regions in dark gray are regions where the steady states are imaginary.

Appendix B. Steady States for Evanescent Coupling

The steady states of Equations (86-90) where $\hat{P}_{s,2} = \hat{P}_{s,1} = \hat{P}_s$ are solved by satisfying

$$0 = \hat{N}_{s,1}R_{s,1} - \eta R_{s,2} \sin(\Theta_s) \quad (136)$$

$$0 = \hat{N}_{s,2}R_{s,2} + \eta R_{s,1} \sin(\Theta_s) \quad (137)$$

$$0 = -\alpha(\hat{N}_{s,2} - \hat{N}_{s,1}) + \eta \cos(\Theta_s) \left(\frac{R_{s,1}}{R_{s,2}} - \frac{R_{s,2}}{R_{s,1}} \right) \quad (138)$$

$$0 = \hat{P}_s - \hat{N}_{s,1} - (1 + 2\hat{N}_{s,1})R_{s,1}^2 \quad (139)$$

$$0 = \hat{P}_s - \hat{N}_{s,2} - (1 + 2\hat{N}_{s,2})R_{s,2}^2. \quad (140)$$

These equations are solved for the steady states by reducing the equations to a system of two equations with the steady state dimensionless excess carrier densities as the variables. After this is accomplished, the new system is solved for the steady state carrier densities. The first step is to solve Equation (136) for $\hat{N}_{s,1}$, Equation (137) for $\hat{N}_{s,2}$, Equation (139) for $R_{s,1}$ and Equation (140) for $R_{s,2}$. This results in

$$\hat{N}_{s,1} = \eta \frac{R_{s,2}}{R_{s,1}} \sin(\Theta_s) \quad (141)$$

$$\hat{N}_{s,2} = -\eta \frac{R_{s,1}}{R_{s,2}} \sin(\Theta_s) \quad (142)$$

$$R_{s,1} = \sqrt{\frac{\hat{P}_s - \hat{N}_{s,1}}{1 + 2\hat{N}_{s,1}}} \quad (143)$$

$$R_{s,2} = \sqrt{\frac{\hat{P}_s - \hat{N}_{s,2}}{1 + 2\hat{N}_{s,2}}}. \quad (144)$$

This shows the steady state carrier densities as functions of steady state amplitudes and the steady state amplitudes as functions of steady state carrier densities. The phase dependence is eliminated by dividing Equation (141) by Equation (142) to arrive at

$$\frac{\hat{N}_{s,1}}{\hat{N}_{s,2}} = -\frac{R_{s,2}^2}{R_{s,1}^2} \quad (145)$$

The first equation that relates $\hat{N}_{s,1}$ to $\hat{N}_{s,2}$ is found by substituting Equations (143, 144) into Equation (145) to arrive at

$$\hat{P}_s(\hat{N}_{s,2} + \hat{N}_{s,1}) + 4\hat{P}_s\hat{N}_{s,2}\hat{N}_{s,1} - (\hat{N}_{s,2}^2 + \hat{N}_{s,1}^2) - 2\hat{N}_{s,2}\hat{N}_{s,1}(\hat{N}_{s,2} + \hat{N}_{s,1}) = 0. \quad (146)$$

In order to find another relation between $\hat{N}_{s,1}$ and $\hat{N}_{s,2}$, the trigonometric identity,

$$\sin^2(\Theta_s) + \cos^2(\Theta_s) = 1, \quad (147)$$

is used. The $\sin^2(\Theta_s)$ is found by solving either Equation (141) or Equation (142) for $\sin(\Theta_s)$, squaring the result, and including Equation (145) where appropriate. The $\cos^2(\Theta_s)$ is found by solving Equation(138) for $\cos(\Theta_s)$, squaring the result, and including Equation (145) where appropriate. The results of this are

$$\sin^2(\Theta_s) = -\frac{\hat{N}_{s,1}\hat{N}_{s,2}}{\eta^2} \quad (148)$$

$$\cos^2(\Theta_s) = \frac{\alpha^2(\hat{N}_{s,2} - \hat{N}_{s,1})^2}{\eta^2\left(-\frac{\hat{N}_{s,2}}{\hat{N}_{s,1}} - \frac{\hat{N}_{s,1}}{\hat{N}_{s,2}} - 2\right)}. \quad (149)$$

Using Equation (147) and Equations (148, 149) a second relation is found.

$$\hat{N}_{s,2}\hat{N}_{s,1} \left((\hat{N}_{s,2} + \hat{N}_{s,1})^2 + \alpha^2(\hat{N}_{s,2} - \hat{N}_{s,1})^2 \right) + \eta^2(\hat{N}_{s,2} + \hat{N}_{s,1})^2 = 0. \quad (150)$$

Equations (146, 150) are now solved for the steady state carrier densities. For simplicity

$$y = \hat{N}_{s,2} + \hat{N}_{s,1} \quad (151)$$

$$x = \hat{N}_{s,2} - \hat{N}_{s,1} \quad (152)$$

are substituted into Equations(146,150) to arrive at

$$0 = \hat{P}_s y + (y^2 - x^2)(\hat{P}_s - \frac{y}{2}) \quad (153)$$

$$0 = \eta^2 y^2 + \frac{y^2 - x^2}{4}(y^2 + \alpha^2 x^2). \quad (154)$$

Equation (153) is now solved for x .

$$x = \pm \sqrt{\frac{y(1+y)(2\hat{P}_s - y)}{1 + 2\hat{P}_s - y}}. \quad (155)$$

Either solution to x from Equation (155) can be substituted into Equation (154) to arrive at

$$\begin{aligned} 0 &= y^5 (1 + \alpha^2) \\ &- y^4 \left((1 - \alpha^2) + 3\hat{P}_s(1 + \alpha^2) + 2\eta^2 \right) \\ &- y^3 \left(4\hat{P}_s\alpha^2 - (\hat{P}_s(1 + \alpha^2) + 4\eta^2)(1 + 2\hat{P}_s) \right) \\ &- y^2 \left(2\eta^2(1 + 2\hat{P}_s)^2 - 2\hat{P}_s^2\alpha^2 \right). \end{aligned} \quad (156)$$

One solution for Equation (156) is $y = 0$ which yields the symmetric steady states. These steady states are

$$\Theta_s = 0 \quad \hat{N}_s = 0 \quad R_s = \sqrt{\hat{P}_s} \quad (157)$$

$$\Theta_s = \pi \quad \hat{N}_s = 0 \quad R_s = \sqrt{\hat{P}_s}, \quad (158)$$

where

$$\hat{N}_s = \hat{N}_{s,1} = \hat{N}_{s,2}, \quad R_s = R_{s,1} = R_{s,2}.$$

The linear stability analysis in Section 3.1 is used to determine if the steady states are stable with the parameters in Table 1, a steady state excess electrical pumping rate from zero to two and a dimensionless coupling strength from 10^{-5} to one. The results

of this analysis are shown in Figure 17. The asymmetric steady states are found

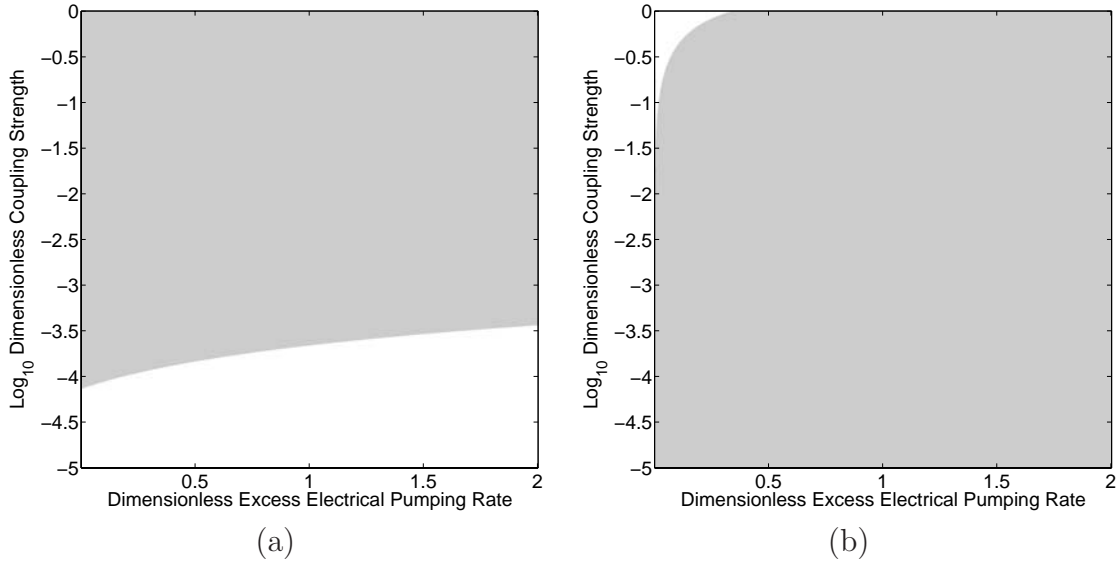


Figure 17. Regions of stability for symmetric steady states of evanescent coupling with symmetric pumping rates and a steady state phase difference of (a) π and (b) 0. Regions in gray are where the steady states are unstable. Regions in white are regions where the steady states are stable.

by solving Equation (156) using the cubic formula found in most algebra references. After solving for y , the solutions are substituted into

$$\hat{N}_{s,1} = \frac{1}{2} \left(y \pm \sqrt{\frac{y(1+y)(2\hat{P}_s - y)}{1 + 2\hat{P}_s - y}} \right) \quad (159)$$

$$\hat{N}_{s,2} = \frac{1}{2} \left(y \mp \sqrt{\frac{y(1+y)(2\hat{P}_s - y)}{1 + 2\hat{P}_s - y}} \right) \quad (160)$$

to find the steady state carrier densities which can then be used to solve for the steady state amplitudes and steady state phase difference. For these steady states to be valid they must be real and stable. For the steady states to be real y must be real as well as a part of the space $((y \leq -1) \cup ((y \geq 0) \cap (y \leq 2\hat{P}_s)) \cup (y > 1 + 2\hat{P}_s))$ to satisfy Equation (155). With this and the linear stability analysis, the steady states either do not exist or are unstable for the parameters in Table 1, a steady state excess

electrical pumping rate from zero to two and a dimensionless coupling strength from 10^{-5} to one. The results of this analysis are shown in Figure 18.

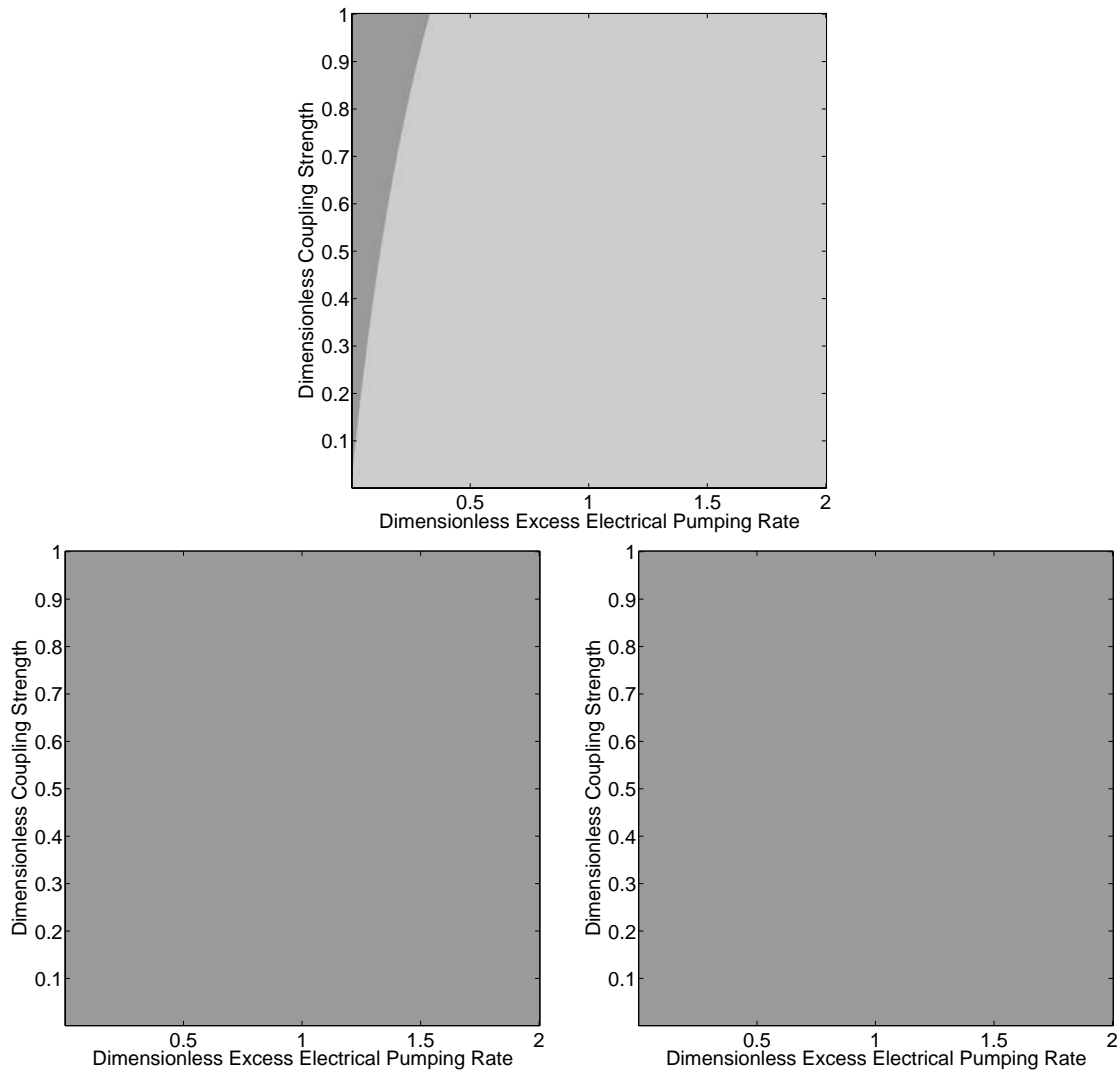


Figure 18. Regions of stability and existence for asynchronous steady states of evanescent coupling with synchronous pumping rates. Regions in gray are where the steady states are unstable. Regions in dark gray are regions where the steady states are imaginary.

Appendix C. *ModulationResponse.m*

This function calculates the infinitesimal modulation response using the procedure in Section 3.2.

```
function [output, J, M0] = ModulationResponse(varargin)

if (strcmp(varargin{1}, 'help'))

    fprintf(1, '[output, J, M0] = ModulationResponse...
(w, h, f, a, b, tp, tc, L, r1, r2, t, n1, n2)\n\n');

    fprintf(1, 'Input:\n');
    fprintf(1, 'w:      Normalized frequencies\n');
    fprintf(1, 'h:      Coupling Strength\n');
    fprintf(1, 'f:      Coupling Phase\n');
    fprintf(1, 'a:      Line-width enhancement factor\n');
    fprintf(1, 'b:      Gain saturation factor\n');
    fprintf(1, 'tp:     Photon Lifetime (ps)\n');
    fprintf(1, 'tc:     Carrier Lifetime (ns)\n');
    fprintf(1, 'L:      Pump phase term (1 for in-phase, -1 for...
out-of-phase)\n');
    fprintf(1, 'r1:     Steady state amplitude in laser 1\n');
    fprintf(1, 'r2:     Steady state amplitude in laser 2\n');
    fprintf(1, 't:      Steady state phase\n');
    fprintf(1, 'n1:     Steady state carrier density in laser 1\n');
    fprintf(1, 'n2:     Steady state carrier density in laser 2\n\n');

    fprintf(1, 'Output:\n');
    fprintf(1, 'output:  Modulation response\n');
    fprintf(1, 'J:       Jacobian matrix\n');
    fprintf(1, 'M0:      Modulation response at zero frequency\n\n\n');
    return;

end

w = varargin{1};
h = varargin{2};
f = varargin{3};
a = varargin{4};
b = varargin{5};
tp = varargin{6};
tc = varargin{7};
L = varargin{8};
```

```

r1 = varargin{9};
r2 = varargin{10};
t = varargin{11};
n1 = varargin{12};
n2 = varargin{13};

T = tc*1000/tp;

s = size(w);
s = s(2);

output = zeros(s,2);

J = [
(1/2)*((1+2*n1)/(1+b*r1^2)-1)-b*(1+2*n1)*r1^2/(1+b*r1^2)^2,
h*cos(t+f),
-r2*h*sin(t+f),
r1/(1+b*r1^2),
0;
h*cos(t-f),
(1/2)*((1+2*n2)/(1+b*r2^2)-1)-b*(1+2*n2)*r2^2/(1+b*r2^2)^2,
-r1*h*sin(t-f),
0,
r2/(1+b*r2^2);
-h*(sin(t-f)/r2-(r2*sin(t+f))/r1^2)-a*b*(1+2*n1)*r1/(1+b*r1^2)^2,
-h*(sin(t+f)/r1-(r1*sin(t-f))/r2^2)+a*b*(1+2*n2)*r2/(1+b*r2^2)^2,
-h*(r1*cos(t-f)/r2 + r2*cos(t+f)/r1),
a/(1+b*r1^2),
-a/(1+b*r2^2);
(-2*(1+2*n1)*r1/(1+b*r1^2)+2*b*(1+2*n1)*r1^3/(1+b*r1^2)^2)/T,
0,
0,
(-1-2*r1^2/(1+b*r1^2))/T,
0;
0,
(-2*(1+2*n2)*r2/(1+b*r2^2)+2*b*(1+2*n2)*r2^3/(1+b*r2^2)^2)/T,
0,
0,
(-1-2*r2^2/(1+b*r2^2))/T];

p = [0; 0; 0; 1/T; L/T];

M0 = abs(inv(J)*(-p));

```

```
for (n = 1:s)
    W = i*w(n)*eye(5);
    M = abs(inv(J-W)*(-p));
    output(n,:) = [10*log10(M(1)/M0(1)), 10*log10(M(2)/M0(2))];
end
return;
```

Appendix D. NUMOR Source Code

This program calculates the non-linear modulation response as outlined in Section 3.3. A sample input file is shown below.

```
Photon Lifetime (ps)          1.600000
Carrier Lifetime (ns)         2.200000
Linewidth Enhancement Factor  5.000000
Gain Saturation Factor        0.000000

Coupling Strength             0.010000
Coupling Phase                0.000000

Pumping Level                 1.056000
Pumping Difference            0.000000
Modulation Amplitude          0.528

High Frequency (GHz)         2.500000
Low Frequency (GHz)          1.000000
Frequency Steps               100
Frequency Periods             100
Time Steps                    10000

Steady States
r1 1.042955
r2 1.042955
t 0.000000
n1 -0.010000
n2 -0.010000
```

"Photon Lifetime" is in picoseconds and "Carrier Density" is in nanoseconds. The "Linewidth Enhancement Factor" is dimensionless. The "Gain Saturation Factor" is the dimensionless gain saturation coefficient. "Coupling Strength" is dimensionless as well as the "Coupling Phase". The "Pumping Level" is the steady state dimensionless excess electrical pumping rate and the "Pumping Difference" is the dimensionless excess electrical pumping rate displacement. The "Modulation Amplitude" is in dimensionless form as well. Frequencies are in gigahertz. "High Frequency" is the highest modulation frequency to calculate and "Low Frequency" is the lowest frequency to calculate with "Frequency Steps" as the integer number of steps in be-

tween. "Frequency Periods" and "Time Steps" control the integration times in the Runge-Kutta algorithm and must be integers.

```

#define _CRT_SECURE_NO_DEPRECATED
#include <stdio.h>
#include <math.h>
#include <conio.h>
#include <time.h>
#include <string.h>
#include <stdlib.h>

//Rate Equations_-----

double R1prime(double n, double beta, double r, double eta, double ri,
               double theta, double phi)
{
    return 0.5*((1+2.0*n)/(1+beta*pow(r,2.0))-1)*r+eta*ri*
           cos(theta+phi);
}

double R2prime(double n, double beta, double r, double eta, double ri,
               double theta, double phi)
{
    return 0.5*((1+2.0*n)/(1+beta*pow(r,2.0))-1)*r+eta*ri*cos(theta-phi);
}

double Tprime(double alpha, double beta, double n2, double n1,
              double eta, double theta, double phi, double r1,
              double r2)
{
    return -(alpha/2.0)*((1+2.0*n2)/(1+beta*pow(r2,2.0))-(1+2.0*n1)/
                       (1+beta*pow(r1,2.0)))-eta*((r1/r2)*sin(theta-phi)+(r2/r1)*
                       sin(theta+phi));
}

double N1prime(double p, double delta, double amp, double f, double t,
               double n, double beta, double r, double T)
{
    return (p-delta+amp*sin(f*t)-n-((1+2.0*n)/(1+beta*pow(r,2.0)))*
           pow(r,2.0))/T;
}

```



```

double N2prime(double p, double delta, double amp, double f, double t,
               double n, double beta, double r, double T, double L)
{
    return (p+delta+L*amp*sin(f*t)-n-((1+2.0*n)/(1+beta*pow(r,2.0)))*
           pow(r,2.0))/T;
}

```

```
//-----
```

```
int main()
{
```

```
//Allocating memory to variables-----
```

```

FILE* input;           //Pointer to input stream
FILE* output;         //Pointer to output stream
double pi = acos(-1.0); //Pi
time_t ti;            //Clock time
char  dump[100];      //Character array dump
double t;             //Normalized time
double dt;           //Time step
int    steps;        //Number of time steps
double p;            //Normalized electrical pumping rate
double amp;          //Amplitude of the electrical modulation
double delta;        //P2 = p + delta, P1 = p - delta
double L;            //1 for in-phase modulation, -1 for out
                    //of phase modulation

double eta;          //Coupling strength
double phi;          //Coupling phase
double taup;         //Photon lifetime
double tauc;         //Carrier lifetime
double T;            //Ratio of Photon lifetime to carrier
                    //lifetime

double alpha;        //Line-width enhancement factor
double beta;         //Gain saturation factor
double f;            //Modulation frequency
double hif;          //High modulation frequency to calculate
double lof;          //Low modulation frequency to calculate
double bw;           //High modulation frequency minus low
                    //modulation frequency

int  periods;        //Number of modulation periods to
                    //calculate

int  fsteps;         //Number of modulation response points to

```

```

        calculate
double real1;      //Real part of the Fourier component of
                   laser1's output
double imag1;     //Imaginary part of the Fourier component
                   of laser1's output
double real2;     //Real part of the Fourier component of
                   laser2's output
double imag2;     //Imaginary part of the Fourier component
                   of laser2's output
double realp;     //Real part of the Fourier component of
                   the pump modulation
double imagp;     //Imaginary part of the Fourier component
                   of the pump modulation
double k1r1;     //Variables for the fourth order
                 Runge-Kutta routine

double k1r2;
double k1t;
double k1n1;
double k1n2;
double k2r1;
double k2r2;
double k2t;
double k2n1;
double k2n2;
double k3r1;
double k3r2;
double k3t;
double k3n1;
double k3n2;
double k4r1;
double k4r2;
double k4t;
double k4n1;
double k4n2;

//-----

//Read input file and initialize variables-----

input = fopen("input.dat", "r");
if (input == NULL)
{
    printf("ERROR: Input file did not open\n");
}

```

```

    printf("\nPress Any Key to Exit");
    getch();
    return 0;
}

fscanf(input, "%s", &dump); fscanf(input, "%s", &dump);
fscanf(input, "%s", &dump);
fscanf(input, "%lf", &taup);
fscanf(input, "%s", &dump); fscanf(input, "%s", &dump);
fscanf(input, "%s", &dump);
fscanf(input, "%lf", &tauc);
fscanf(input, "%s", &dump); fscanf(input, "%s", &dump);
fscanf(input, "%s", &dump);
fscanf(input, "%lf", &alpha);
fscanf(input, "%s", &dump); fscanf(input, "%s", &dump);
fscanf(input, "%s", &dump);
fscanf(input, "%lf", &beta);

T = tauc*1000/taup;

fscanf(input, "%s", &dump); fscanf(input, "%s", &dump);
fscanf(input, "%lf", &eta);
fscanf(input, "%s", &dump); fscanf(input, "%s", &dump);
fscanf(input, "%lf", &phi);

fscanf(input, "%s", &dump); fscanf(input, "%s", &dump);
fscanf(input, "%lf", &p);
fscanf(input, "%s", &dump); fscanf(input, "%s", &dump);
fscanf(input, "%lf", &delta);
fscanf(input, "%s", &dump); fscanf(input, "%s", &dump);
fscanf(input, "%lf", &amp);

fscanf(input, "%s", &dump); fscanf(input, "%s", &dump);
fscanf(input, "%s", &dump);
fscanf(input, "%lf", &hif);
fscanf(input, "%s", &dump); fscanf(input, "%s", &dump);
fscanf(input, "%s", &dump);
fscanf(input, "%lf", &lof);
fscanf(input, "%s", &dump); fscanf(input, "%s", &dump);
fscanf(input, "%i", &fsteps);
fscanf(input, "%s", &dump); fscanf(input, "%s", &dump);
fscanf(input, "%i", &periods);
fscanf(input, "%s", &dump); fscanf(input, "%s", &dump);

```

```

fscanf(input, "%i", &steps);

bw = hif - lof;

//Amplitude of laser 1 output
double* r1 = (double*)calloc(steps+1, sizeof(double));
//Amplitude of laser 2 output
double* r2 = (double*)calloc(steps+1, sizeof(double));
//Phase
double* theta = (double*)calloc(steps+1, sizeof(double));
//Carrier density in laser 1
double* n1 = (double*)calloc(steps+1, sizeof(double));
//Carrier density in laser 2
double* n2 = (double*)calloc(steps+1, sizeof(double));
//Pump modulation
double* dp = (double*)calloc(steps+1, sizeof(double));

fscanf(input, "%s", &dump); fscanf(input, "%s", &dump);
fscanf(input, "%s", &dump);
fscanf(input, "%lf", &r1[1]);
fscanf(input, "%s", &dump);
fscanf(input, "%lf", &r2[1]);
fscanf(input, "%s", &dump);
fscanf(input, "%lf", &theta[1]);
fscanf(input, "%s", &dump);
fscanf(input, "%lf", &n1[1]);
fscanf(input, "%s", &dump);
fscanf(input, "%lf", &n2[1]);

fclose(input);

//-----
//Double check-----

printf("Photon Lifetime:           %f (ps)\n", taup);
printf("Carrier Lifetime:           %f (ns)\n", tauc);
printf("Linewidth Enhancement Factor: %f\n", alpha);
printf("Gain Saturation Factor:       %f\n\n", beta);

printf("Coupling Strength:             %f \n", eta);
printf("Coupling Phase:               %f \n\n", phi);

```

```

printf("Pumping Level:                %f\n",  p);
printf("Pumping Difference:           %f\n",  delta);
printf("Modulation Amplitude:         %f\n\n", amp);

printf("High Frequency:                %f (GHz)\n", hif);
printf("Low Frequency:                 %f (GHz)\n", lof);
printf("Frequency Steps:                %i\n",    fsteps);
printf("Frequency Periods:             %i\n",    periods);
printf("Time Steps:                    %i\n\n",    steps);

printf("Steady States\n");
printf("r1:  %f\n",  r1[1]);
printf("r2:  %f\n",  r2[1]);
printf("t:   %f\n",  theta[1]);
printf("n1:  %f\n",  n1[1]);
printf("n2:  %f\n\n", n2[1]);

printf("Are these correct? (Y/N): ");
scanf("%s", dump);
if (strncmp(dump, "n", 1) == 0)
{
    printf("\nPress Any Key to Exit");
    getch();
    return 0;
}

printf("\nOut of Phase? (Y/N): ");
scanf("%s", dump);
if (strncmp(dump, "y", 1) == 0)
{
    L = -1.0;
}
else
{
    L = 1.0;
}

//-----
//Start the clock-----

time(&ti);

```

```

//-----
//Initializing output stream-----

output = fopen("output.dat", "w");
if (output == NULL)
{
    printf("ERROR: Output file did not open\n");
    printf("\nPress Any Key to Exit");
    getch();
    return 0;
}

fprintf(output, "Frequency (GHz)\tModulation Response (dB)\t
            Modulation Response (dB)\n");

//-----

//Scanning modulation frequencies-----

for (int m = 0; m <= fsteps; m++)
{
    printf("\nFrequency Point %i/%i\n", m, fsteps);

    f = (lof + m*bw/fsteps)*taup*0.001;
    dt = periods/(f*steps);
    f = 2.0*pi*f;
    t = 0.0;

//Fourth order Runge-Kutta routine-----

for (int n = 2; n <= steps+1; n++)
{
    k1r1 = dt*R1prime(n1[n-1], beta, r1[n-1], eta,
                    r2[n-1], theta[n-1], phi);
    k1r2 = dt*R2prime(n2[n-1], beta, r2[n-1], eta,
                    r1[n-1], theta[n-1], phi);
    k1t = dt*Tprime(alpha, beta, n2[n-1], n1[n-1], eta,
                    theta[n-1], phi, r1[n-1], r2[n-1]);
    k1n1 = dt*N1prime(p, delta, amp, f, t, n1[n-1], beta,
                    r1[n-1], T);
    k1n2 = dt*N2prime(p, delta, amp, f, t, n2[n-1], beta,
                    r2[n-1], T, L);
}
}

```

```

k2r1 = dt*R1prime(n1[n-1] + 0.5*k1n1, beta,
                  r1[n-1] + 0.5*k1r1, eta, r2[n-1] + 0.5*k1r2,
                  theta[n-1] + 0.5*k1t, phi);
k2r2 = dt*R2prime(n2[n-1] + 0.5*k1n2, beta,
                  r2[n-1] + 0.5*k1r2, eta, r1[n-1] + 0.5*k1r1,
                  theta[n-1] + 0.5*k1t, phi);
k2t  = dt*Tprime(alpha, beta, n2[n-1] + 0.5*k1n2,
                  n1[n-1] + 0.5*k1n1, eta, theta[n-1] + 0.5*k1t,
                  phi, r1[n-1] + 0.5*k1r1, r2[n-1] + 0.5*k1r2);
k2n1 = dt*N1prime(p, delta, amp, f, t + dt/2,
                  n1[n-1] + 0.5*k1n1, beta, r1[n-1] + 0.5*k1r1,
                  T);
k2n2 = dt*N2prime(p, delta, amp, f, t + dt/2,
                  n2[n-1] + 0.5*k1n2, beta, r2[n-1] + 0.5*k1r2,
                  T, L);

k3r1 = dt*R1prime(n1[n-1] + 0.5*k2n1, beta,
                  r1[n-1] + 0.5*k2r1, eta, r2[n-1] + 0.5*k2r2,
                  theta[n-1] + 0.5*k2t, phi);
k3r2 = dt*R2prime(n2[n-1] + 0.5*k2n2, beta,
                  r2[n-1] + 0.5*k2r2, eta, r1[n-1] + 0.5*k2r1,
                  theta[n-1] + 0.5*k2t, phi);
k3t  = dt*Tprime(alpha, beta, n2[n-1] + 0.5*k2n2,
                  n1[n-1] + 0.5*k2n1, eta, theta[n-1] + 0.5*k2t,
                  phi, r1[n-1] + 0.5*k2r1, r2[n-1] + 0.5*k2r2);
k3n1 = dt*N1prime(p, delta, amp, f, t + dt/2,
                  n1[n-1] + 0.5*k2n1, beta, r1[n-1] + 0.5*k2r1,
                  T);
k3n2 = dt*N2prime(p, delta, amp, f, t + dt/2,
                  n2[n-1] + 0.5*k2n2, beta, r2[n-1] + 0.5*k2r2,
                  T, L);

k4r1 = dt*R1prime(n1[n-1] + k3n1, beta,
                  r1[n-1] + k3r1, eta, r2[n-1] + k3r2,
                  theta[n-1] + k3t, phi);
k4r2 = dt*R2prime(n2[n-1] + k3n2, beta,
                  r2[n-1] + k3r2, eta, r1[n-1] + k3r1,
                  theta[n-1] + k3t, phi);
k4t  = dt*Tprime(alpha, beta, n2[n-1] + k3n2,
                  n1[n-1] + k3n1, eta, theta[n-1] + k3t, phi,
                  r1[n-1] + k3r1, r2[n-1] + k3r2);
k4n1 = dt*N1prime(p, delta, amp, f, t + dt,

```

```

        n1[n-1] + k3n1, beta, r1[n-1] + k3r1, T);
k4n2 = dt*N2prime(p, delta, amp, f, t + dt,
        n2[n-1] + k3n2, beta, r2[n-1] + k3r2, T, L);

r1[n]    = r1[n-1] + (k1r1 + 2.0*k2r1 + 2.0*k3r1 +
                    k4r1)/6.0;
r2[n]    = r2[n-1] + (k1r2 + 2.0*k2r2 + 2.0*k3r2 +
                    k4r2)/6.0;
theta[n] = theta[n-1] + (k1t + 2.0*k2t + 2.0*k3t +
                    k4t)/6.0;
n1[n]    = n1[n-1] + (k1n1 + 2.0*k2n1 + 2.0*k3n1 +
                    k4n1)/6.0;
n2[n]    = n2[n-1] + (k1n2 + 2.0*k2n2 + 2.0*k3n2 +
                    k4n2)/6.0;
dp[n]    = amp*sin(f*(t + dt));

t = t + dt;

printf("Percent Complete:  %3.0i\r", n*100/(steps+1));
}

//-----

//Calculate Fourier component-----

real1 = 0.0;
imag1 = 0.0;
real2 = 0.0;
imag2 = 0.0;
realp = 0.0;
imagp = 0.0;

for (int l = 1; l <= steps+1; l++)
{
    real1 = real1 + r1[l]*cos(2.0*pi*periods*(l-1)/
        (steps+1));
    imag1 = imag1 + r1[l]*sin(2.0*pi*periods*(l-1)/
        (steps+1));
    real2 = real2 + r2[l]*cos(2.0*pi*periods*(l-1)/
        (steps+1));
    imag2 = imag2 + r2[l]*sin(2.0*pi*periods*(l-1)/
        (steps+1));
    realp = realp + dp[l]*cos(2.0*pi*periods*(l-1)/

```



```

                (steps+1));
    imagp = imagp + dp[l]*sin(2.0*pi*periods*(l-1)/
                (steps+1));
}
//-----

//Print to output stream-----

fprintf(output, "%le\t%le\t%le\n", lof + m*bw/fsteps,
    10.0*log10(sqrt(pow(real1, 2.0) + pow(imag1, 2.0))
                /sqrt(pow(realp, 2.0) + pow(imagp, 2.0))),
    10.0*log10(sqrt(pow(real2, 2.0) + pow(imag2, 2.0))
                /sqrt(pow(realp, 2.0) + pow(imagp, 2.0))));

//-----

}

//-----

//Calculate run time, close the output stream, and end the program-----

printf("\n\nThis run took %.0f seconds to complete\n",
    difftime(time(NULL), ti));

fclose(output);
printf("\nPress Any Key to Exit");
getch();

return 0;

//-----
}

```

Appendix E. SteadyState.m

This function calculates steady states using Newton's method as outlined in Section 4.2.1. The initial guess is the symmetric steady states with user specified initial steady state phase difference. The Newton's method algorithm terminates when the steady states are reached, when the tolerance is met or when the maximum number of iterations is exceeded. The stability of these states is determined using the linear stability analysis in Section 3.1, and the user is informed if they are stable or not. Finally the user is prompted if he wants to create an input file using the calculated steady states for the program that calculates the non-linear modulation response.

```
function [output, evalues] = SteadyState(varargin)
s = size(varargin);
s = s(2);

if ((s ==1)&&(strcmp(varargin{1}, 'help')))
    fprintf(1, '[output, evalues] = SteadyState...
    (h, f, p, d, a, b, tp, tc, t)\n\n');
    fprintf(1, 'Input\n');
    fprintf(1, 'h:      Coupling Strength\n');
    fprintf(1, 'f:      Coupling Phase\n');
    fprintf(1, 'p:      Average pump level\n');
    fprintf(1, 'd:      Pump difference\n');
    fprintf(1, 'a:      Line-width enhancement factor\n');
    fprintf(1, 'b:      Gain saturation factor\n');
    fprintf(1, 'tp:     Photon Lifetime (ps)\n');
    fprintf(1, 'tc:     Carrier Lifetime (ns)\n');
    fprintf(1, 't:      Steady state phase starting point\n\n');
    fprintf(1, 'Output:\n');
    fprintf(1, 'output:  Steady States\n');
    fprintf(1, 'evalues: Eigenvalues of the Jacobian matrix\n\n');
    fprintf(1, 'Tags:\n');
    fprintf(1, 'MaxIterations: Set maximum number of iterations\n');
    fprintf(1, 'Tolerance:     Set tolerance level\n\n');
    return;
end

if ((s == 10)|| (s == 12)|| (s < 9)|| (s > 13))
    fprintf(1, 'Improper number of input arguments. \n');
    return;
end
```

```

h = varargin{1};
f = varargin{2};
p = varargin{3};
d = varargin{4};
a = varargin{5};
b = varargin{6};
tp = varargin{7};
tc = varargin{8};
t = varargin{9};

T = tc*1000/tp;

if (s == 9)
    tol = 1.0e-6;
    maxit = 100;
end

if (s == 11)
    if (strcmp(varargin{10}, 'MaxIterations'))
        maxit = varargin{11};
        tol = 10e-6;
    elseif (strcmp(varargin{10}, 'Tolerance'))
        tol = varargin{11};
        maxit = 100;
    else
        fprintf(1, '%"s" is an improper tag. \n', varargin{10});
        return;
    end
end

if (s == 13)
    if (strcmp(varargin{10}, 'MaxIterations'))
        maxit = varargin{11};
        tol = varargin{13};
    elseif (strcmp(varargin{10}, 'Tolerance'))
        tol = varargin{11};
        maxit = varargin{13};
    else
        fprintf(1, '%"s" is an improper tag. \n', varargin{10});
        return;
    end
end
end

```

```

n1 = (b*p - 2*h*cos(t + f))/(2 + b);
n2 = (b*p - 2*h*cos(t - f))/(2 + b);
r1 = sqrt((p - n1)/(1 + 2*n1 - b*(p - n1)));
r2 = sqrt((p - n2)/(1 + 2*n2 - b*(p - n2)));

R1prime = inline('(1/2)*((1+2*n)/(1+b*r^2)-1)*r + h*ri*cos(t+f)',...
    'n', 'b', 'r', 'h', 'ri', 't', 'f');
R2prime = inline('(1/2)*((1+2*n)/(1+b*r^2)-1)*r + h*ri*cos(t-f)',...
    'n', 'b', 'r', 'h', 'ri', 't', 'f');
Tprime = inline('-(a/2)*((1+2*n2)/(1+b*r2^2)-(1+2*n1)/(1+b*r1^2))...
    -h*(r1*sin(t-f)/r2 + r2*sin(t+f)/r1)',...
    'a', 'b', 'n2', 'n1', 'h', 't', 'f', 'r1', 'r2');
N1prime = inline('p - d - n - ((1+2*n)/(1+b*r^2))*r^2',...
    'p', 'd', 'n', 'b', 'r');
N2prime = inline('p + d - n - ((1+2*n)/(1+b*r^2))*r^2',...
    'p', 'd', 'n', 'b', 'r');

for (n = 1:maxit)

    J = [ (1/2)*((1+2*n1)/(1+b*r1^2)-1)-b*(1+2*n1)*r1^2/(1+b*r1^2)^2,
        h*cos(t+f),
        -r2*h*sin(t+f),
        r1/(1+b*r1^2),
        0;
        h*cos(t-f),
        (1/2)*((1+2*n2)/(1+b*r2^2)-1)-b*(1+2*n2)*r2^2/(1+b*r2^2)^2,
        -r1*h*sin(t-f),
        0,
        r2/(1+b*r2^2);
        -h*(sin(t-f)/r2-(r2*sin(t+f))/r1^2)-a*b*(1+2*n1)*r1/(1+b*r1^2)^2,
        -h*(sin(t+f)/r1-(r1*sin(t-f))/r2^2)+a*b*(1+2*n2)*r2/(1+b*r2^2)^2,
        -h*(r1*cos(t-f)/r2 + r2*cos(t+f)/r1),
        a/(1+b*r1^2),
        -a/(1+b*r2^2);
        (-2*(1+2*n1)*r1/(1+b*r1^2)+2*b*(1+2*n1)*r1^3/(1+b*r1^2)^2)/T,
        0,
        0,
        (-1-2*r1^2/(1+b*r1^2))/T,
        0;
        0,
        (-2*(1+2*n2)*r2/(1+b*r2^2)+2*b*(1+2*n2)*r2^3/(1+b*r2^2)^2)/T,
        0,
        0
    ];

```

```

0,
(-1-2*r2^2/(1+b*r2^2))/T];

F = [R1prime(n1, b, r1, h, r2, t, f);
      R2prime(n2, b, r2, h, r1, t, f);
      Tprime(a, b, n2, n1, h, t, f, r1, r2);
      N1prime(p, d, n1, b, r1);
      N2prime(p, d, n2, b, r2)];

dif = inv([1,0,0,0,0;0,1,0,0,0;0,0,1,0,0;0,0,0,T,0;0,0,0,0,T])*J)*F;

r1 = r1 - dif(1);
r2 = r2 - dif(2);
t = t - dif(3);
n1 = n1 - dif(4);
n2 = n2 - dif(5);

if (sqrt(dif*dif') < tol)

    fprintf(1, 'Steady states reached within tolerance at ...
              iteration: %i \n\n', n-1);
    output = [r1, r2, t, n1, n2];
    break;

elseif (n == maxit)

    output = [r1, r2, t, n1, n2];
    fprintf(1, 'Maximum number of iterations was reached before ...
              tolerance was met. \n\n');

end

end

evalues = eig(J);

if ((real(evalues(1)) <= 0)&&(real(evalues(2)) <= 0)&&...
    (real(evalues(3)) <= 0)&&(real(evalues(4)) <= 0)&&...
    (real(evalues(5)) <= 0))

    fprintf(1, 'The steady states are stable\n\n');

else

```

```

    fprintf(1, 'The steady states are unstable\n\n');

end

fprintf(1, 'Steady States\n');
fprintf(1, '%f\n', output);
str = input('\nCreate a NUMOR input file (y/n): ', 's');

if (strcmp(str, 'y'))

    fid = fopen('input.dat', 'w');
    if (fid == -1)
        fprintf(1, '\nERROR: Input file failed to open\n')
        return;
    end

    fprintf(fid, 'Photon Lifetime (ps)           %f\n', tp);
    fprintf(fid, 'Carrier Lifetime (ns)           %f\n', tc);
    fprintf(fid, 'Linewidth Enhancement Factor %f\n', a);
    fprintf(fid, 'Gain Saturation Factor %f\n\n', b);
    fprintf(fid, 'Coupling Strength %f\n', h);
    fprintf(fid, 'Coupling Phase %f\n\n', f);
    fprintf(fid, 'Pumping Level %f\n', p);
    fprintf(fid, 'Pumping Difference %f\n', d);
    fprintf(fid, 'Modulation Amplitude \n\n');
    fprintf(fid, 'High Frequency (GHz) \n');
    fprintf(fid, 'Low Frequency (GHz) \n');
    fprintf(fid, 'Frequency Steps \n');
    fprintf(fid, 'Frequency Periods \n');
    fprintf(fid, 'Time Steps \n\n');
    fprintf(fid, 'Steady States\n');
    fprintf(fid, 'r1 %f\n', r1);
    fprintf(fid, 'r2 %f\n', r2);
    fprintf(fid, 't %f\n', t);
    fprintf(fid, 'n1 %f\n', n1);
    fprintf(fid, 'n2 %f', n2);

    fclose(fid);

end

return;

```

Bibliography

1. G. Wilson, R. DeFreez, and H. Winful, "Modulation of phased-array semiconductor lasers at K-band frequencies," *IEEE J. of Quantum Electronics*, vol. 27, no. 6, pp. 1696–1704, 1991.
2. G. Agrawal, "Coupled-cavity semiconductor lasers under current modulation: Small-signal analysis," *IEEE J. of Quantum Electronics*, vol. 21, no. 3, pp. 255–263, 1985.
3. S. Tang and J. Liu, "Chaos synchronization in semiconductor lasers with optoelectronic feedback," *IEEE J. of Quantum Electronics*, vol. 39, no. 6, pp. 708–715, 2003.
4. J. Mork, B. Tromborg, and J. Mark, "Chaos in semiconductor lasers with optical feedback: Theory and experiment," *IEEE J. of Quantum Electronics*, vol. 28, no. 1, pp. 93–108, 1992.
5. H. Matsueda, "AlGaAs OEIC transmitters," *IEEE J. of Lightwave Technology*, vol. 5, no. 10, pp. 1382–1390, 1987.
6. G. Wilson, R. DeFreez, and H. Winful, "Modulation of twin-emitter semiconductor lasers beyond the frequency of relaxation oscillations," *Optics Communications*, vol. 82, no. 3,4, pp. 293–298, 1991.
7. P. Acedo, H. Lamela, B. Roycroft, G. Carpintero, and R. Santos, "High bandwidth small signal modulation response of two laterally mode-locked diode lasers," *IEEE Photonics Technology Letters*, vol. 14, no. 8, pp. 1055–1057, 2002.
8. Y. Li, N. Naderi, V. Kovanis, and L. Lester, "Modulation response of an injection-locked 1550nm quantum dash semiconductor laser." To be published, LEOS 2007.
9. H. Lamela, M. Leones, G. Carpintero, C. Simmendinger, and O. Hess, "Analysis of the dynamic behavior and short-pulse modulation scheme for laterally coupled diode lasers," *IEEE J. on Selected Topics in Quantum Electronics*, vol. 7, no. 2, pp. 192–200, 2001.

10. D. Grasso, D. Serkland, G. Peake, K. Geib, and K. Choquette, "Direct modulation characteristics of composite resonator vertical-cavity lasers," *IEEE J. of Quantum Electronics*, vol. 42, no. 12, pp. 1248–1254, 2006.
11. A. Hohl, A. Gavrielides, T. Erneaux, and V. Kovanis, "Quasiperiodic synchronization for two delay-coupled semiconductor lasers," *Physical Review A*, vol. 59, no. 5, pp. 3941–3949, 1999.
12. A. Hohl, A. Gavrielides, T. Erneaux, and V. Kovanis, "Localized synchronization in two coupled nonidentical semiconductor lasers," *Physical Review Letters*, vol. 78, no. 25, pp. 4745–4748, 1997.
13. G. Agrawal and N. Dutta, *Semiconductor Lasers*. Van Nostrand Reinhold, second ed., 1993.
14. S. Chuang, *Physics of Optoelectronic Devices*. John Wiley & Sons, Inc., 1995.
15. C. Henry, "Theory of the linewidth of semiconductor lasers," *IEEE J. of Quantum Electronics*, vol. 18, no. 2, pp. 259–264, 1982.
16. R. Lang and K. Kobayashi, "External optical feedback effects on semiconductor injection laser properties," *IEEE J. of Quantum Electronics*, vol. 16, no. 3, pp. 347–355, 1980.
17. S. Yanchuk, K. Schneider, and L. Recke, "Dynamics of two mutually coupled semiconductor lasers: Instantaneous coupling limit," *Physical Review E*, vol. 69, pp. 1–12, 2004.
18. H. Winful and S. Wang, "Stability of phase locking in coupled semiconductor laser arrays," *Applied Physics Letters*, vol. 53, no. 20, pp. 1894–1896, 1988.
19. D. Nichols and H. Winful, "The effect of nonlinear gain on the stability of evanescently coupled semiconductor laser arrays," *Journal of Applied Physics*, vol. 73, no. 1, pp. 459–461, 1993.
20. B. Saleh and M. Teich, *Fundamentals of Photonics*. John Wiley & Sons, Inc., second ed., 2007.

21. J. Verdeyen, *Laser Electronics*. Prentice Hall, third ed., 1995.
22. P. Alsing, V. Kovanis, A. Gavrielides, and T. Erneux, “Lang and Kobayashi phase equation,” *Physical Review A*, vol. 53, no. 6, pp. 4429–4434, 1996.
23. D. Botez and D. Scifres, eds., *Diode Laser Arrays*, vol. 14 of *Cambridge Studies in Modern Optics*. Cambridge University Press, 1994.
24. R. Burden and J. Faires, *Numerical Analysis*. Thomson Brooks/Cole, eighth ed., 2005.
25. T. Perez, A. Scire, G. V. der Sande, P. Colet, and C. Mirasso, “Bistability and all-optical switching in semiconductor ring lasers,” *Optics Express*, vol. 15, no. 20, pp. 12941–12948, 2007.
26. P. Varangis, A. Gavrielides, T. Erneux, V. Kovanis, and L. Lester, “Frequency entrainment in optically injected semiconductor lasers,” *Physical Review Letters*, vol. 78, no. 12, pp. 2353–2356, 1997.

REPORT DOCUMENTATION PAGE

Form Approved
OMB No. 0704-0188

The public reporting burden for this collection of information is estimated to average 1 hour per response, including the time for reviewing instructions, searching existing data sources, gathering and maintaining the data needed, and completing and reviewing the collection of information. Send comments regarding this burden estimate or any other aspect of this collection of information, including suggestions for reducing the burden, to the Department of Defense, Executive Service Directorate (0704-0188). Respondents should be aware that notwithstanding any other provision of law, no person shall be subject to any penalty for failing to comply with a collection of information if it does not display a currently valid OMB control number.

PLEASE DO NOT RETURN YOUR FORM TO THE ABOVE ORGANIZATION.

1. REPORT DATE (DD-MM-YYYY) 27-03-2008	2. REPORT TYPE Master's Thesis	3. DATES COVERED (From - To) June 2007-March 2008
---	-----------------------------------	--

4. TITLE AND SUBTITLE Modulation Response of Twin Optically Coupled Diode Lasers	5a. CONTRACT NUMBER
	5b. GRANT NUMBER
	5c. PROGRAM ELEMENT NUMBER

6. AUTHOR(S) Golden, Eric M. Captain, USAF	5d. PROJECT NUMBER
	5e. TASK NUMBER
	5f. WORK UNIT NUMBER

7. PERFORMING ORGANIZATION NAME(S) AND ADDRESS(ES) Air Force Institute of Technology Graduate School of Engineering and Management (AFIT/EN) 2950 Hobson Way WPAFB, OH 45433-7765	8. PERFORMING ORGANIZATION REPORT NUMBER AFIT/GAP/ENP/08-M05
---	---

9. SPONSORING/MONITORING AGENCY NAME(S) AND ADDRESS(ES) AFRL/RYP Dr. Vassilios Kovanis 2241 Avionics Circle, Area B Bldg 620 WPAFB, OH 45433 674-9943	10. SPONSOR/MONITOR'S ACRONYM(S)
	11. SPONSOR/MONITOR'S REPORT NUMBER(S)

12. DISTRIBUTION/AVAILABILITY STATEMENT
APPROVED FOR PUBLIC RELEASE; DISTRIBUTION UNLIMITED

13. SUPPLEMENTARY NOTES

14. ABSTRACT
The modulation response of twin optically coupled diode lasers is investigated by modeling the dynamics of the system with a set of single mode rate equations. Steady states of the system are derived analytically or calculated numerically when an analytic expression is not easily available. The stability of the steady states is examined by using a linear stability analysis, which is also used in an algorithm that calculates the infinitesimal modulation response. The modulation response is also calculated by using a numerical method that directly integrates the rate equations. Typical parameters for an InGaAsP diode laser are used in the algorithms to investigate mutual coupling and evanescent coupling. It is discovered that mutually coupled lasers can be effectively modulated out to frequencies of approximately 9 GHz compared to 4 GHz for a solitary laser. Large regions of the parameter space for evanescent coupling produce unstable steady states, but this is remedied by introducing asymmetric DC currents through the lasers or by introducing the effects of gain saturation. With stable steady states, evanescently coupled lasers can be effectively modulated at frequencies out to about 30 GHz which is more than a seven fold improvement over a solitary laser.

15. SUBJECT TERMS
Frequency Response, Diode Lasers, Laser Arrays, Coupling, Dynamics

16. SECURITY CLASSIFICATION OF:			17. LIMITATION OF ABSTRACT	18. NUMBER OF PAGES	19a. NAME OF RESPONSIBLE PERSON
a. REPORT U	b. ABSTRACT U	c. THIS PAGE U			Maj. Thomas Niday, AFIT/ENP 19b. TELEPHONE NUMBER (Include area code) (937)255-3636ext4828 thomas.niday@afit.edu